Proteome plasticity during Physcomitrium patens spore germination – from the desiccated phase to heterotrophic growth and reconstitution of photoautotrophy

Lea Hembach, Philipp W Niemeyer, Kerstin Schmitt, Jaccoline M S Zegers, Patricia Scholz, Dennis Brandt, Janis J Dabisch, Oliver Valerius, Gerhard H Braus, Markus Schwarzländer, et al.

the plant journal

SEB SOCIETY FOR EXPERIMENTAL BIOLOGY

The Plant Journal (2024) **117**, 1466–1486 doi: 10.1111/tpj.16574

Proteome plasticity during *Physcomitrium patens* spore germination – from the desiccated phase to heterotrophic growth and reconstitution of photoautotrophy

Lea Hembach[1,†], Philipp W. Niemeyer[2,†], Kerstin Schmitt[3], Jaccoline M. S. Zegers[4], Patricia Scholz[5], Dennis Brandt[6], Janis J. Dabisch[1], Oliver Valerius[3], Gerhard H. Braus[3], Markus Schwarzländer[6], Jan de Vries[4], Stefan A. Rensing[7,8,‡] and Till Ischebeck[1,2,*]

[1]*Green Biotechnology, Institute of Plant Biology and Biotechnology (IBBP), University of Münster, 48143 Münster, Germany,*
[2]*Department of Plant Biochemistry, Albrecht-von-Haller-Institute for Plant Sciences and Göttingen Center for Molecular Biosciences (GZMB), University of Göttingen, 37077 Göttingen, Germany,*
[3]*Department for Molecular Microbiology and Genetics, Genetics and Göttingen Center for Molecular Biosciences (GZMB) and Service Unit LCMS Protein Analytics, Institute for Microbiology, University of Göttingen, 37077 Göttingen, Germany,*
[4]*Department of Applied Bioinformatics, Göttingen Center for Molecular Biosciences (GZMB) and Campus Institute Data Science (CIDAS), Institute for Microbiology and Genetics, University of Göttingen, 37077 Göttingen, Germany,*
[5]*Laboratoire Reproduction et Développement des Plantes (RDP), UCB Lyon 1, CNRS, INRAE, Université de Lyon, ENS de Lyon, Lyon, France,*
[6]*Plant Energy Biology, Institute of Plant Biology and Biotechnology (IBBP), University of Münster, 48143 Münster, Germany,*
[7]*Plant Cell Biology, Department of Biology, University of Marburg, Marburg, Germany,*
[8]*BIOSS Centre for Biological Signalling Studies, University of Freiburg, Freiburg, Germany*

Received 7 August 2023; revised 13 November 2023; accepted 22 November 2023; published online 7 December 2023.
*For correspondence (e-mail till.ischebeck@uni-muenster.de).
†Equal contribution.
‡Present address: Faculty of Chemistry and Pharmaceutical Sciences, University of Freiburg, Freiburg, Germany

SUMMARY

The establishment of moss spores is considered a milestone in plant evolution. They harbor protein networks underpinning desiccation tolerance and accumulation of storage compounds that can be found already in algae and that are also utilized in seeds and pollen. Furthermore, germinating spores must produce proteins that drive the transition through heterotrophic growth to the autotrophic plant. To get insight into the plasticity of this proteome, we investigated it at five timepoints of moss (*Physcomitrium patens*) spore germination and in protonemata and gametophores. The comparison to previously published Arabidopsis proteome data of seedling establishment showed that not only the proteomes of spores and seeds are functionally related, but also the proteomes of germinating spores and young seedlings. We observed similarities with regard to desiccation tolerance, lipid droplet proteome composition, control of dormancy, and β-oxidation and the glyoxylate cycle. However, there were also striking differences. For example, spores lacked any obvious storage proteins. Furthermore, we did not detect homologs to the main triacylglycerol lipase in Arabidopsis seeds, SUGAR DEPENDENT1. Instead, we discovered a triacylglycerol lipase of the oil body lipase family and a lipoxygenase as being the overall most abundant proteins in spores. This finding indicates an alternative pathway for triacylglycerol degradation via oxylipin intermediates in the moss. The comparison of spores to *Nicotiana tabacum* pollen indicated similarities for example in regards to resistance to desiccation and hypoxia, but the overall developmental pattern did not align as in the case of seedling establishment and spore germination.

Keywords: ***Physcomitrium patens*, spore, spore germination, seeds, lipid droplets, proteome, LEA proteins, *Arabidopsis thaliana*.**

INTRODUCTION

Bryophytes are non-vascular land plants comprising mosses, liverworts, and hornworts. Seminal phylogenomic work over the last years suggests them to be a monophyletic group (Leebens-Mack et al., 2019; Li et al., 2020; Puttick et al., 2018). Representing one of the two major lineages of land plants, bryophytes are key for inferring traits present in the last common ancestor of land plants and understanding the plant terrestrialization event that occurred about 500 million years ago (Kenrick, 2017; Ligrone et al., 2012; Rensing, 2018). Already before terrestrialization, streptophyte algae, the paraphylum that nowadays includes the closest relatives to the land plants, were likely able to form desiccation-tolerant cells, including akinetes, pre-akinetes, and zygospores (Herburger et al., 2015; McLean & Pessoney, 1971; Pichrtová et al., 2014). Furthermore, zygospores of filamentous Zygnematophyceae have resilient coating rich in aromatics (resembling sporopollenin) and accumulate lipids and starch (Permann et al., 2021, 2022). It is, therefore, likely that such structures occurred in the algal progenitors of land plants. Under this scenario, mosses then evolved haploid single-cell structures called spores as part of their sexual reproductive life cycle—possibly through co-option of the resilient structures that occurred in their algal progenitors.

These spores represented a decisive advantage on land, as they are able to fully desiccate and persist for extended periods before germinating under favorable conditions. The first tissue that develops from the spore is a filamentous network, the protonemata (Cove, 2005) that are already photosynthetically active and later give rise to leafy gametophores. After the formation of sexual organs, fertilization, and meiosis, spores are produced within a capsule to complete the life cycle (Engel, 1968; Nakosteen & Hughes, 1978; Rensing et al., 2020).

These spores display functional and structural resemblances with the reproductive tissues of seed plants, seeds, and pollen, which have been present in the plant kingdom since the evolution of spermatophytes (Huang et al., 2009; Loconte & Stevenson, 1990). Similar to pollen, spores are less-intricate structures, small-sized, haploid, and protected by a sporopollenin wall (Daku et al., 2016; Wallace et al., 2011). However, spores are the primary means of dispersal in the moss life cycle, and in this sense, they are functionally similar to spermatophyte seeds (Vesty et al., 2016). Similar to spores, pollen and seeds of most species exhibit desiccation-tolerant characteristics, and share with spores certain molecular and gene expression patterns (Gaff & Oliver, 2013; Matilla, 2022; Oliver et al., 2000).

One important element of desiccation-tolerant tissues is the accumulation of late embryogenesis abundant (LEA) proteins as a protective measure against dehydration and other abiotic stressors such as temperature and salt stress (Artur et al., 2019; Cuming et al., 2007; Delahaie et al., 2013; Saavedra et al., 2006). These highly hydrophilic LEA proteins contain intrinsically disordered regions and are classified into eight multigene families in plants (Artur et al., 2019). The protective functions facilitated by LEA proteins include the vitrification of the cytosol in cooperation with non-reducing sugars. When the organism is subjected to desiccation, a glassy state is established by replacing water with a hydrophilic protein shell (Manfre et al., 2008; Wolkers et al., 2001). Furthermore, LEA proteins demonstrate anti-aggregation (Chakrabortee et al., 2012) and chaperone-like properties (Kovacs et al., 2008) and can also regulate membrane permeability (Liu et al., 2009). The role of distinct LEA proteins is functionally multifaceted; however, and only a subpopulation of LEAs is thought to contribute to desiccation tolerance (Artur et al., 2019; Matilla, 2022).

Another shared feature of most spores, seeds, and pollen is the accumulation of neutral lipids such as triacylglycerol (TAG), which are stored in cytosolic lipid droplets (LDs) (Guzha et al., 2023). LDs may enhance desiccation resilience by maintaining membrane integrity through filling the intracellular space, which counteracts cell shrinkage and prevents membrane collapse (Lyall & Gechev, 2020). The induction of LD formation might derive from a generic, ancient, abiotic stress-related machinery that originated even before embryophytes emerged on *terra firma* (de Vries & Ischebeck, 2020). In spores and seeds, lipid droplets serve as an energy and carbon source for post-germinative growth (Huang et al., 2009; Ischebeck et al., 2020), while in pollen, their main function might be to serve as an acyl-chain source during pollen tube formation and growth (Ischebeck, 2016; Müller & Ischebeck, 2018) as well as a carbon sink during pollen tube growth (Krawczyk et al., 2022). A hallmark of lipid droplets embedded in desiccation-tolerant tissues is their outer coverage with oleosin (Murphy et al., 1995). This integral surface protein is likely to shield the droplets and inhibits their coalescence during desiccation (Siloto et al., 2006), potentially through electrostatic repulsion arising from their negative charge (Huang, 1992).

The accumulation of such proteins with protective functions requires an underlying regulatory network. In this context, the plant hormone abscisic acid (ABA) has a crucial role in the acquisition of desiccation tolerance (Cuming, 2019). ABSCISIC ACID INSENSITIVE 3 (ABI3) is a key transcription factor activated by ABA (Khandelwal et al., 2010). ABA serves as a trigger and component of a signaling pathway highly conserved in land plants (Oliver et al., 2005). This includes inducing the expression of oleosins (Crowe et al., 2000; Yang et al., 2022) and several LEA proteins (Tian et al., 2020), among other gene products related to dehydration. Moreover, ABI3 is essential for acquiring desiccation tolerance in Arabidopsis seeds

(Giraudat et al., 1992) and ABA inducible vegetative desiccation tolerance in the moss *Physcomitrium patens* (Arif et al., 2019; Khandelwal et al., 2010).

P. patens has gained particular importance as a model for non-seed plants over the past decades (Cove, 2005; Rensing et al., 2020; Shaw et al., 2011). In 2008, the *P. patens* genome was the first of any bryophyte to be fully sequenced (Rensing et al., 2008).

Making use of this genetic resource, several proteomic datasets were acquired in the last two decades giving insights into abiotic stress and desiccation tolerance-associated proteins in protonema and gametophores (Cho et al., 2006; Cui et al., 2012; Luo et al., 2020; Mamaeva et al., 2022; Sarnighausen et al., 2004; Skripnikov et al., 2009; Toshima et al., 2014; Wang et al., 2010; Wang, Yang, Zhang, et al., 2009; Wang, Yang, Liu, et al., 2009; Wang et al., 2008; Yotsui et al., 2016).

To understand key strategies of developmental rather than adaptive desiccation tolerance followed by rehydration, we devised a comprehensive proteomic analysis of spores, germinating spores, protonemata, and gametophores of the *P. patens* ecotype Reute (Hiss et al., 2017). A comparison to Arabidopsis seedling establishment provides remarkable insight into the operation of several shared protein networks required for desiccation tolerance. Furthermore, we could extend the similarities of spores and seeds to the transition phase leading to photoautotrophy in both organisms.

RESULTS

The *P. Patens* spore proteome changes during germination and is distinct from vegetative tissues

Several studies indicated that the molecular programs and the protein networks first described as characteristics of seeds have evolved much earlier and also occur in non-seed plants (de Vries & Ischebeck, 2020; Farrant et al., 2009; Huang et al., 2009; López-Pozo et al., 2018; Oliver et al., 2000, 2005). In order to get insight into conserved mechanisms and players we chose a lineage that (i) has separated from the seed plant lineage before (orthodox) seeds evolved and (ii) shares key physiological characteristics, such as sudden metabolic activation after quiescence and desiccation, the storage of a large number of LDs and their degradation during the transition to the autotrophic phase. We chose *P. patens* spore germination as a tangible model and devised a proteomic approach of five stages of spore germination (0, 8, 24, 48, and 72 h after rehydration) and two vegetative stages (protonema and gametophore) of the moss (Figure 1a) and compared it to the previously published proteomes of Arabidopsis seeds and seedlings (Kretzschmar et al., 2020), and *Nicotiana tabacum* microspores, pollen and pollen tubes (Ischebeck et al., 2014) that were reanalyzed for this study from the original raw data files.

LC–MS/MS analysis of five independent biological replicates of each *P. patens* stage was performed after a tryptic digest of the protein samples and all protein groups were quantified using the label-free MS1-based algorithm of MaxQuant (intensity-based absolute quantification, iBAQ). These values were then divided by the total iBAQ of the respective sample and multiplied by 1000, resulting in relative iBAQ (riBAQ) values. All *P. patens* library entries were then functionally annotated by performing a BLASTp search against the Arabidopsis TAIR10 primary transcript protein release database (Data S1; Lamesch et al., 2012). In total, 3447 protein groups could be identified and quantified (Data S2a). 2609 of these protein groups were identified based on two peptides and were found in at least three samples of one of the stages (Data S2b). These rigidly filtered protein groups were further analyzed. While it was not possible to completely remove the residues of the spore capsules, the dynamics of the proteome dataset over time (Figure 1, Data S2) indicates that the contamination is not very strong.

For studying the proteome in all stages investigated of *P. patens*, a principal component analysis (PCA, Figure 1b) was generated. The PCA indicates that the proteomes between spores and vegetative stages differ the most, while the first three spore stages are closely related. The similarities between the individual biological replicates demonstrate the high reproducibility of the measurements.

Next, for each protein, averages were calculated for each developmental stage. These were normalized setting the value of the developmental stage with the highest value to 1. These values were then hierarchically clustered (Figure 1c; Data S3). Several clusters comprise proteins that are high in early spore stages (clusters 3–5 and 8), while others contain proteins found predominantly during late spore germination (clusters 1, 2, 6, and to some extent 7, 17, 18) or in the protonema and gametophore tissues (cluster 28 and 30). Among the proteins enriched in spores that are quickly degraded during spore germination (cluster 4, Figure 1d) are a homolog to the phytochrome B type photoreceptor HY3 that plays a role in the regulation of de-etiolation of Arabidopsis seedlings (Wester et al., 1994), and the RNA helicase LOS4 (LOW EXPRESSION OF OSMOTICALLY RESPONSIVE GENES 4) that is involved in mRNA exports and acts upstream of abiotic stress responses (Gong et al., 2005). Another example is a putative β-d-xylosidase. Homologs of this protein in Arabidopsis are involved in cell wall loosening by removing xylose and arabinose side chains from cell wall components such as rhamnogalacturonan I (Arsovski et al., 2009; Guzha et al., 2022).

Two small heat shock proteins contained in cluster 5 first rise in abundance and then sharply drop (Figure 1d). Homologs of these proteins are important for seed vigor and longevity in Arabidopsis and are ABA-regulated (Waters & Vierling, 2020). Other proteins in the clusters that increased during spore germination but were much lower in protonema and gametophores are involved in β-oxidation (for example, multifunctional protein in cluster

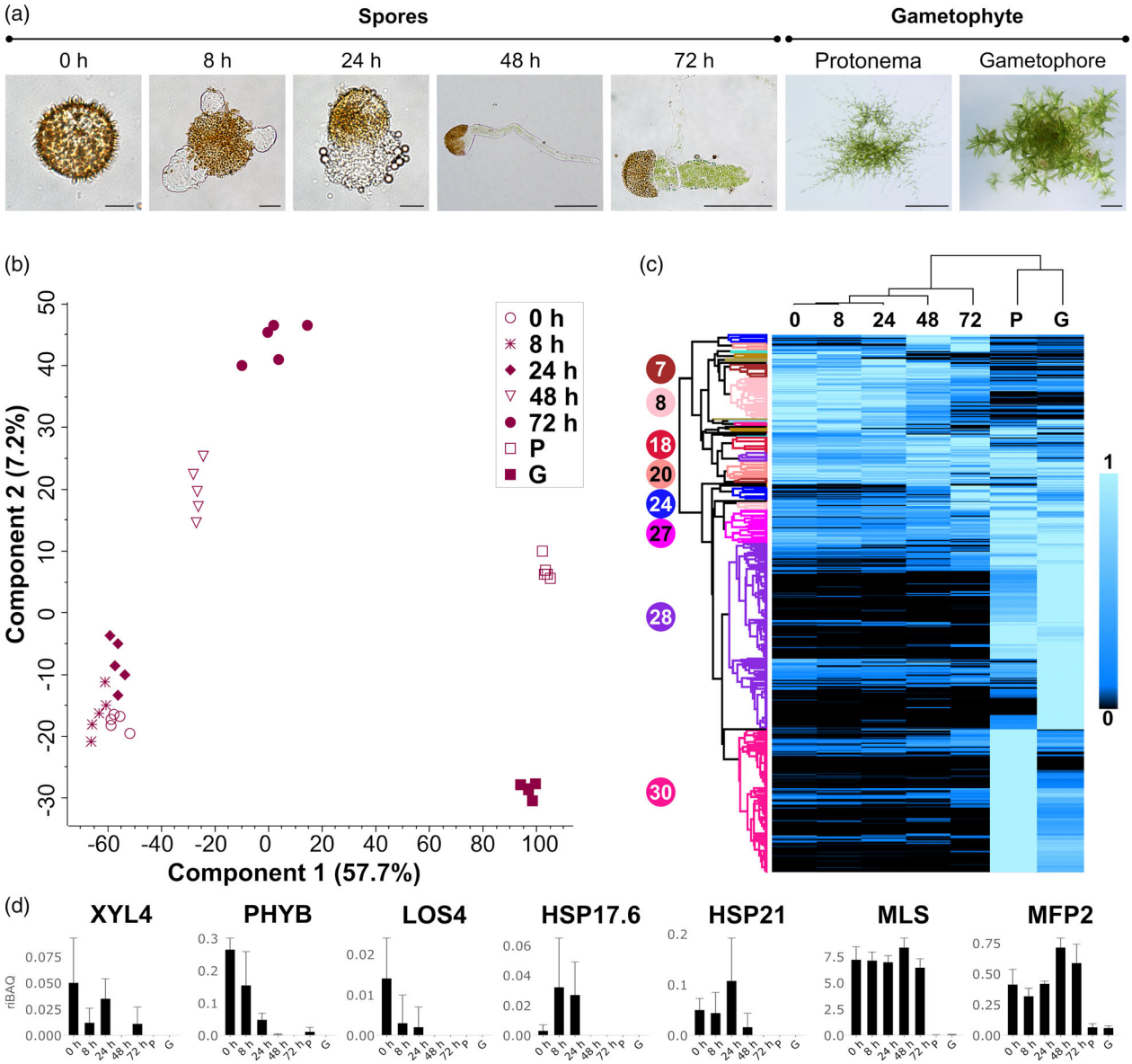

Figure 1. Proteomic analysis of seven developmental stages of *P. patens*. (a) Micrographs of developmental stages analyzed in this study: germinating spores of *P. patens* ecotype Reute 0–72 fter rehydration, juvenile protonema and adult gametophores. First chloronema cells emerge after 8 h, continuously growing over the time course. Size bars, 0, 8, 24 ≙ 10 μm; 48, 72 ≙ 50 μm; protonema ≙ 1 mm, gametophores ≙ 2 mm. (b) Principal component analysis plot (n = 5 per stage). (c) Hierarchical clustering of the means (n = 5 per stage), with the highest mean of each protein group being set to 1. Proteins sorted by clusters can be found in Data S3. Clusters with more than 50 candidates are labeled with numbers. (d) Exemplary proteins enriched in spores that are homolgous to the Arabidopsis proteins BETA-D-XYLOSIDASE4 (XYL4), HY3/PHYTOCHROME B (PHYB), LOW EXPRESSION OF OSMOTICALLY RESPONSIVE GENES 4 (LOS4), HEAT SHOCK PROTEIN 17.6 and 21 (HSP 17.6 and 21), MALATE SYNTHASE (MLS), and MULTIFUNCTIONAL PROTEIN 2 (MFP2).

18) and the glyoxylate cycle (such as malate synthase in cluster 7) indicating that protein synthesis and conversion of TAG into carbohydrates are especially high in spores 48 and 72 h old.

GO term analysis highlights similarities between *P. Patens* spore germination and Arabidopsis seedling establishment

In order examine the involvement of the detected proteins in larger cellular processes, these proteins were assigned to their respective homologs in Arabidopsis (Data S1) before being categorized and combined to Gene Ontology (GO) Terms published for Arabidopsis (Berardini et al., 2004). While the *P. patens* proteins might have a different function than their homologs in Arabidopsis, the overall assessment can indicate how certain pathways or protein networks change throughout development. For this, the riBAQ values of all proteins of each GO Term were added and compared to previously published data of Arabidopsis seeds and seedlings (Data S4; Kretzschmar

et al., 2020) and *N. tabacum* microspores, pollen and pollen tubes (Data S5–S7, Ischebeck et al., 2014). For the second comparison, we performed a BLASTp search of all *N. tabacum* proteins against the proteomes of Arabidopsis and *P. patens* to assign homologs (Data S5) and reanalyzed the original raw data using the same work flow as for *P. patens* (Data S6).

Several distribution patterns of protein abundances (riBAQ) consolidated in GO terms are consistent between germinating *P. patens* spores and Arabidopsis seedling establishment (Figure 2). Examples are the GO terms "Response to abscisic acid," "Lipid droplet," "Oxylipin biosynthetic process," and "Maintenance of seed dormancy," which display their highest abundance spores and seeds, and then decline. An increase in protein abundance during spore germination and seedling establishment, respectively, was observed for the GO terms "Response to hydrogen-peroxide," Protein folding," "Glyoxylate cycle," and "Fatty acid beta-oxidation." The values for these terms then dropped in protonemata and gametophores and 60 h old seedlings, respectively. High in these later stages were proteins assigned to the GO terms "Reductive pentose phosphate activity" and "Photosynthesis."

Conversely, certain ontogenetic patterns related to GO terms of seeds and spores show apparent dissimilarities. For example, the terms "Pollen development" and "Seed development" manifest a gradual decline in germinating spores. In contrast, values for these terms in Arabidopsis nearly double from rehydrated seeds to the 36 h seedling stage, and subsequently decrease again after 60 h to rehydrated seed baseline levels. Moreover, the GO term "Cellular response to hypoxia" shows a relatively stable abundance in germinating spores, while being almost entirely abolished in seedlings.

Nevertheless, despite the notable differences in the ontogenetic patterns between spores and seeds, certain critical developmental steps are shared by both types of structures. These similarities may be linked to desiccation tolerance, oil degradation, and the transition into the vegetative photosynthetically active tissue important in both seeds and spores. The proteins of the different stages of *N. tabacum* pollen development (with a focus on two predesiccated stages, dry pollen, and pollen tubes) were also assigned to GO terms according to their homology to Arabidopsis proteins (Data S5) and their abundancies were added (Figure 2; Data S7). In this dataset, similarities to spores can also be seen. For example, proteins associated with the GO terms seed development, and responses water deprivation, abscisic acid and hypoxia were also highest in dry pollen similar to dry spores. Strong differences were observed in the terms "Lipid droplet" and "Glyoxylate cycle" that were magnitudes lower in all pollen stages.

A quantitative comparison supports the similarities between the seed and spore proteomes

In order to quantitatively compare spore germination and seedling establishment, the two proteomic datasets of *P. patens* (excluding protonema and gametophores) and Arabidopsis (Kretzschmar et al., 2020), the *P. patens* protein groups were assigned to the closest homolog present in the Arabidopsis dataset (E-value $\leq 10^{-5}$, Data S1b and S8a) based on a BLASTp search. If several Arabidopsis protein groups were assigned to the same *P. patens* accession, the values were added (Data S8b). Then, the averages for each stage were calculated and the highest average of each of the two datasets was set to 1. Proteins only found in one dataset were removed (Data S8c). All samples of *P. patens* were analyzed in direct comparison

GO ID	GO Term	*P. patens*							*A. thaliana*			*N. tabacum*			
		0 h	8 h	24 h	48 h	72 h	P	G	RS	36 h	60 h	PM	BP	DP	PT
GO:0009737	Response to abscisic acid	114	104	97.3	76.0	38.2	14.3	15.8	616	336.9	189.3	26.4	48.5	65.7	51.5
GO:0005811	Lipid droplet	87.1	79.4	73.1	52.8	23.7	0.2	0.4	13.4	4.9	1.9	0.29	0.7	0.24	0.24
GO:0009555	Pollen development	70.4	63.8	57.2	38.4	17.2	11.6	10.4	4.6	7.4	4.0	12.6	21.6	31.9	36.3
GO:0048316	Seed development	102	93.2	87.3	64.3	34.0	9.8	8.9	1.3	2.0	1.7	25.1	36.2	40.1	26.9
GO:0031408	Oxylipin biosynthetic process	96.1	88.4	78.6	53.3	24.2	4.9	6.0	5.3	3.6	2.6	3.9	1.0	0.60	0.26
GO:0006096	Glycolytic process	26.4	25.2	22.6	23.3	14.9	16.6	20.8	19.0	32.8	45.7	37.5	87.1	92.0	97.5
GO:0009414	Response to water deprivation	107	98.7	92.9	70.5	36.0	15.2	27.9	5.4	12.1	10.4	38.7	39.2	69.8	36.0
GO:0010231	Maintenance of seed dormancy	19.3	21.2	18.9	15.8	8.4	1.0	4.2	3.3	0.8	0.1	0.00	0.04	0.04	0.09
GO:0071456	Cellular response to hypoxia	35.7	38.2	37.8	33.9	25.0	6.5	17.8	0.001	0.006	0.009	11.3	31.3	48.5	37.5
GO:0042542	Response to hydrogen peroxide	89.5	113	123	102	77.9	4.2	2.6	12.7	12.0	7.2	11.2	14.2	21.4	17.2
GO:0006457	Protein folding	115	136	146	132	105.7	33.7	28.7	18.5	41.5	36.9	82.7	90.6	61.4	46.0
GO:0006097	Glyoxylate cycle	7.7	7.7	8.2	12.9	9.6	0	0.1	1.7	31.7	11.8	0.08	0.18	0.10	0.13
GO:0006635	Fatty acid beta-oxidation	3.6	3.1	3.7	8.0	10.0	1.5	1.2	1.9	6.1	3.9	2.4	2.8	5.3	4.6
GO:0019253	Reductive pentose-phosphate cycle	3.1	2.6	3.4	5.7	12.6	41.4	37.3	4.6	54.4	180	2.7	1.9	0.5	1.4
GO:0015979	Photosynthesis	4.2	3.5	3.0	5.0	23.2	89.5	79.8	1.1	36.4	108	0.82	2.3	0.8	2.7

Figure 2. Abundance of proteins in selected GO terms. Depicted are averaged ($n = 5$) and summed relative iBAQ values (in ‰ of total protein abundance) of all proteins assigned to the corresponding GO term for each individual tissue type. For *P. patens*, the 5 stages of spore germination (0, 8, 24, 48, 72 h), as well as protonema (P) and gametophores (G) are displayed, compared to three stages of Arabidopsis seedling establishment and four stages of *N. tabacum* pollen development originally published in Kretzschmar et al. (2020) and Ischebeck et al. (2014), respectively. Given are rehydrated seeds (RS), seedlings grown for 36 and 60 h, polarized microspores (PM), bicellular pollen (BP), dry pollen (DP) and pollen tubes (PT).

to samples of Arabidopsis of rehydrated (RS), stratified (StS), and 24, 36, 48, or 60 h germinated seeds (Kretzschmar et al., 2020) normalized in the same manner.

A PCA plot of this analysis (Figure 3a) displayed a separation of the developmental stages by component 1 that was similar in both species. However, component 2 strongly separated 0 h spores and 0 h seeds. Hierarchical clustering (Figure 3b, Data S9) displayed that spores of 0–24 h are most closely related to seeds, 48 h spores to 24 and 36 h old seedlings, and 72 h spores to seedlings at 48 and 60 h. Furthermore, the clustering of the proteins showed that spores and seeds contain a subset of very similar protein sets. Clusters 4–7, for example, harboring proteins of high abundance in both seeds and spores that decrease over time, contain a total of 105 proteins that might be evolutionarily conserved in protecting desiccated stages or facilitating the early phase of the transition from a heterotrophic offspring dispersal stage to an autotrophic plant. Proteins in these clusters might be involved in cell wall-related metabolism, such as a putative xylosidase/arabinosidase (cluster 4, Data S9) and several putative galactose oxidases (cluster 7). Further examples are heat shock proteins of the 17.6 kd family and so-called universal stress proteins (USPs, all cluster 6) that are associated with diverse biotic and abiotic stress responses (Chi et al., 2019). Our analysis of this cluster further highlighted proteins that are so far of unknown function but might have a conserved function in seeds and spores.

We also took a closer look at proteins in cluster 27 that were high in 36–48 h old Arabidopsis seedlings and 36 h old germinated spores, as these proteins might be involved in the late transition phase to autotrophy. This cluster contains numerous proteins involved in protein synthesis, such as tRNA synthases, translation initiation factors, and ribosomal proteins, indicating an increased rate during this time window in both seedlings and germinating spores.

We also compared the developmental pattern of protein abundance between spore germination and *N. tabacum* late pollen development and pollen tube growth in the same manner as described for spores and seeds above (Data S10). The PCA of this comparison, however, showed no similarities between the spore and pollen stages with component 1 separating only the *N. tabacum* stages, and component 2 the ones of *P. patens* (Figure 3c). Hierarchical clustering gave a similar result, as the samples of the two species formed each a cluster of their own with the exception of the polarized microspores and the 72 h spores that were most distant to all other samples (Figure 3d).

Spores are enriched in LD and LEA proteins and proteins involved in oxylipin metabolism

A one-on-one comparison of all developmental stages from *P. patens* (Figure S1) using imputed values (Data S11a) revealed significantly changed protein abundances between all stages except for the comparison of the 0 and 8 h time points. To get further insight into proteins with specific importance in spores, we compared the proteome of 0 h spores to 72 h old germinated spores and gametophores (Figure 4; Data S11b,c).

Two proteins much higher in 0 h versus 72 h spores might play a role in detoxifying oxidized lipids and their downstream products (Data S11b). They are homologs to the proteins CeQORH (CHLOROPLAST ENVELOPE QUINONE OXIDOREDUCTASE HOMOLOG, At4g13010) and CHLADR (CHLOROPLAST ALDEHYDE REDUCTASE, At1g54870) that have been implicated in such functions in Arabidopsis plastids (Curien et al., 2016; Yamauchi et al., 2011). Both these proteins are found in dry seeds and are degraded during seedling establishment (Kretzschmar et al., 2020).

A similar pattern in the seedling establishment is observed for an AWPM-19-like membrane family protein (AT1G04560). A *P. patens* homolog was strongly enriched in spores in comparison to gametophores (Data S11c), and the Arabidopsis gene is highly expressed in seeds (Klepikova et al., 2016) while a homolog in rice has been shown to be involved in ABA transport (Yao et al., 2018).

The comparisons furthermore displayed that the spores at 0 h were chiefly enriched in proteins homologous to (i) LEA (late embryogenesis abundant) proteins, (ii) known LD proteins (Guzha et al., 2023), and (iii) proteins involved in oxylipin metabolism. These proteins will be described below.

Late embryogenesis proteins show distinct expression patterns suggestive of evolutionary conservation

Two of the 14 detected LEA proteins stayed high during spore germination and were almost absent in vegetative tissues, while two further isoforms were highest in gametophores (Figure 5; Data S12). However, most of the LEAs detected in this study were highest in spores, degraded within 72 h, and largely absent in protonema and gametophores. A similar decrease was observed for Arabidopsis LEAs during seedling establishment (Kretzschmar et al., 2020) and in pollen tubes in comparison to dry pollen (Data S6).

As LEA proteins appear to be important in both seeds and spores, we investigated the evolutionary history of LEAs across 24 species in the green line to get a deeper understanding of this class of proteins. To this end, we put a focus on four species – *A. thaliana, Oriza sativa, Cyperus esculentus, P. patens* – for which we also analyzed experimental protein and transcript data from several different datasets (see Experimental Procedures section for details).

In a phylogenetic tree of all LEA families of the 24 species, the individual eight multigene LEA families cluster in separate clades. We could not pinpoint the common

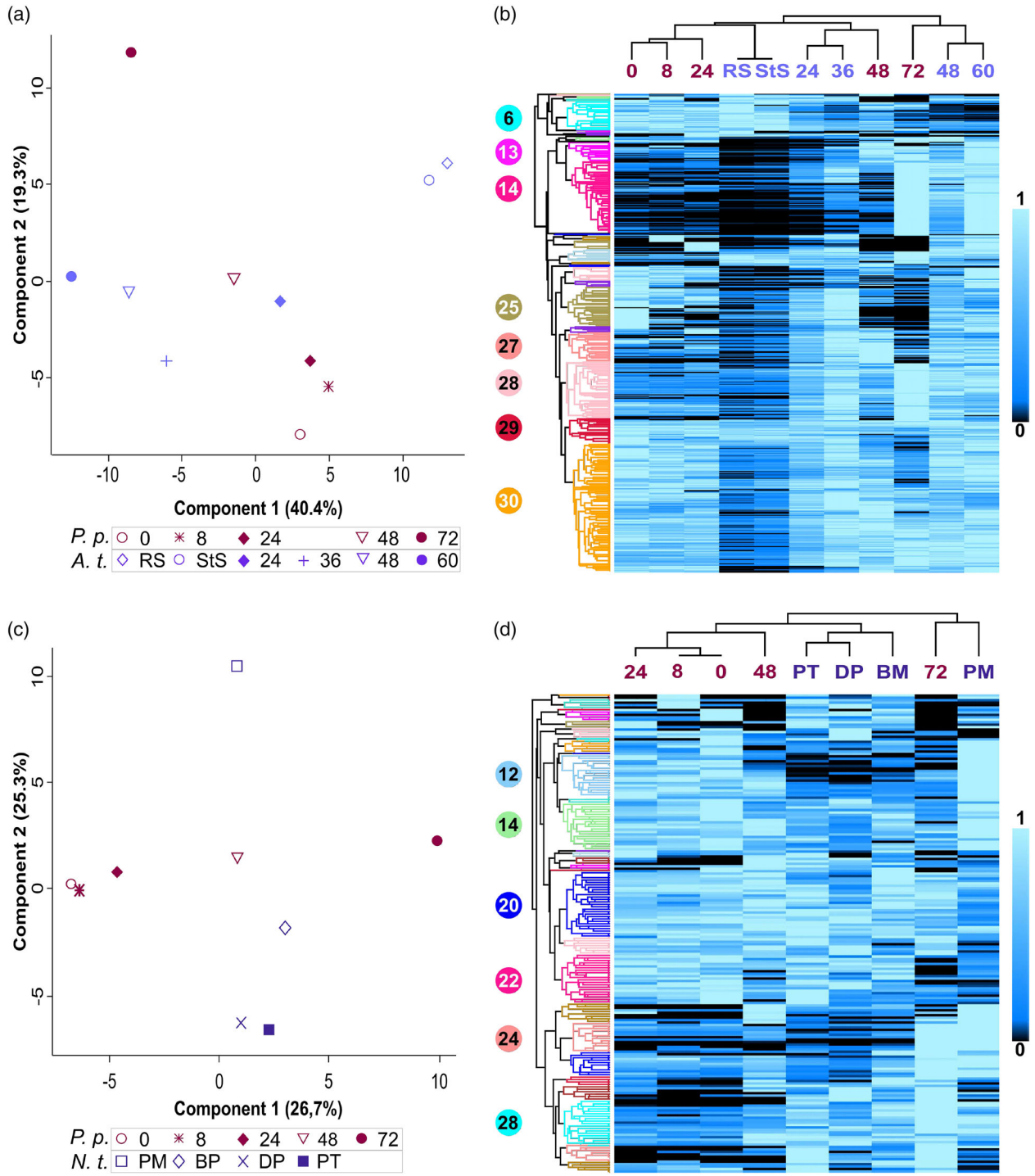

Figure 3. Comparison of *P. patens* spore germination to Arabidopsis seedling establishment and *N. tabacum* pollen development. For *P. patens*, the 5 stages of spore germination (0, 8, 24, 48, 72 h) for Arabidopsis (a, b) rehydrated seeds (RS), stratified seeds (StS), 24, 36, 48, and 60 h of seedling establishment, and for *N. tabacum* (c, d) polarized microspores (PM), bicellular pollen (BP), dry pollen (DP) and pollen tubes (PT) are displayed. The highest mean of each protein (averaged values with $n = 5$) was set to 1 individually for *P. patens* and Arabidopsis. (a, c) Principal component analysis plots. (b, d) Hierarchical cluster of which all proteins are sorted by clusters can be found in Data S9 and S10c; clusters with more than 50 candidates are labeled with numbers. Arabidopsis and *N. tabacum* data were originally published in Kretzschmar et al. (2020) and Ischebeck et al. (2014), respectively.

ancestral proteins prior to diversification into all of the diverse LEA families (Figure S2). That said, both LEA_5 and LEA_4 groups are conserved across all analyzed species, suggesting that these two groups may be the evolutionary oldest (Figure S2). LEA_4 presents the most diverse group with the most different subcellular localizations (Figure 6).

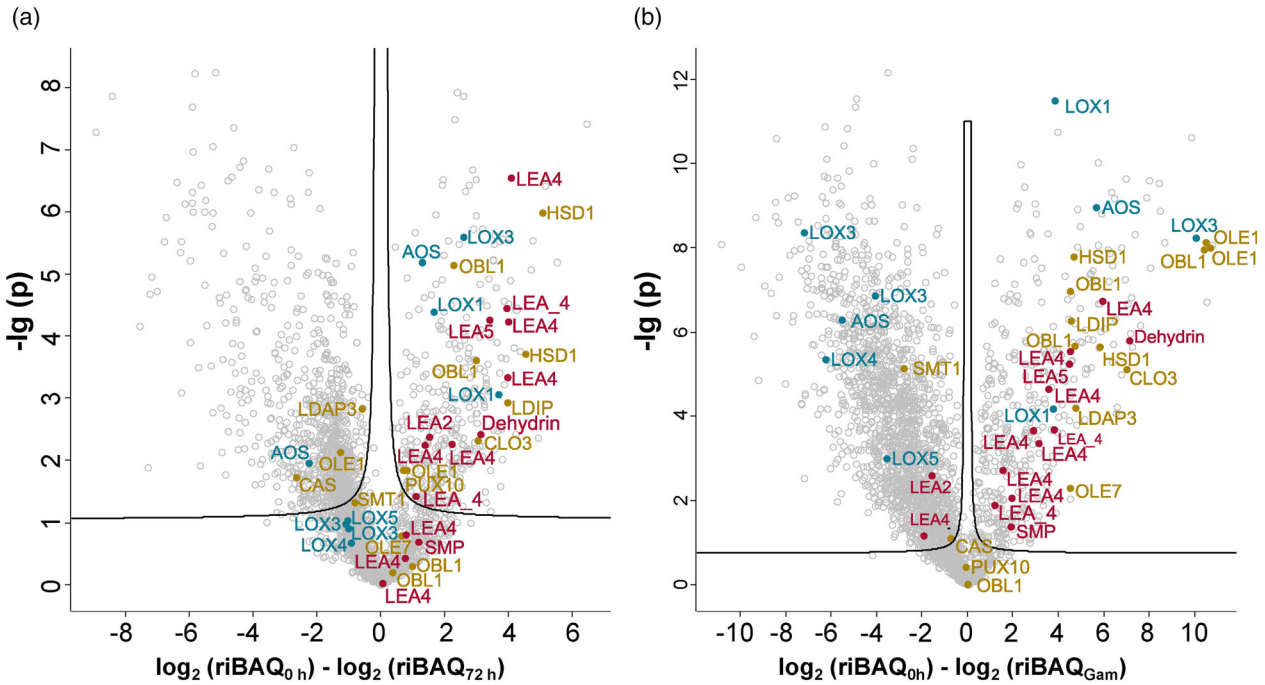

Figure 4. Volcano plots visualize differences between 0 h spores and 72 h spores (a), and between 0 h spores and gametophores (b). The log_2 transformed and imputed data were compared and p-values calculated. Yellow circles represent homologs of known LD proteins, magenta circles LEA proteins, and blue circles oxylipin-related proteins. The black line indicates a false discovery rate of 0.05. AOS, allene oxide synthase; CAS, cycloartenol synthase; CLO, caleosin; LEA, late embryogenesis abundant protein; LOX, lipoxygenase; HSD, steroleosin; LDAP, lipid droplet-associated protein; LDIP, LDAP-interacting protein; OBL, oil body lipase; OLE, oleosin; PUX, plant UBX domain-containing protein; SMP, seed maturation protein; SMT, sterol methyltransferase.

(a)

Cluster	*P. patens* ID	*A. thaliana* ID	Family	0 h	8 h	24 h	48 h	72 h	P	G
5	Pp3c6_200V3	AT5G27980	SMP	0.06	0.06	0.09	0.01	0.03	0.00	0.01
7	Pp3c4_18020V3	AT1G72100	LEA_4	0.03	0.03	0.03	0.04	0.00	0.00	0.00
8	Pp3c5_11880V3	AT1G20440	Dehydrin	0.87	1.19	1.13	0.58	0.14	0.00	0.00
8	Pp3c3_12260V3	AT1G72100	LEA_4	0.22	0.15	0.08	0.05	0.00	0.02	0.01
8	Pp3c16_20740V3	AT2G40170	LEA_5	0.22	0.27	0.30	0.21	0.00	0.00	0.00
8	Pp3c24_1540V3	AT3G53040	LEA_4	0.03	0.04	0.02	0.01	0.00	0.00	0.00
8	Pp3c23_14420V3	AT3G53040	LEA_4	0.30	0.35	0.27	0.20	0.01	0.05	0.01
8	Pp3c12_22320V3	AT3G53040	LEA_4	0.65	0.59	0.46	0.23	0.05	0.00	0.00
8	Pp3c15_15760V3	AT3G53040	LEA_4	0.19	0.16	0.12	0.08	0.01	0.01	0.01
8	Pp3c8_16760V3	AT5G44310	LEA_4	0.09	0.07	0.05	0.02	0.01	0.02	0.00
18	Pp3c12_22320V3	AT1G52690	LEA_4	0.20	0.12	0.18	0.16	0.24	0.00	0.02
18	Pp3c4_880V3	AT3G15670	LEA_4	0.07	0.05	0.09	0.08	0.09	0.02	0.01
28	Pp3c24_14840V3	AT2G44060	LEA_2	0.33	0.35	0.12	0.13	0.11	0.59	0.91
28	Pp3c4_23110V3	AT3G53040	LEA_4	0.02	0.02	0.02	0.01	0.00	0.08	0.14

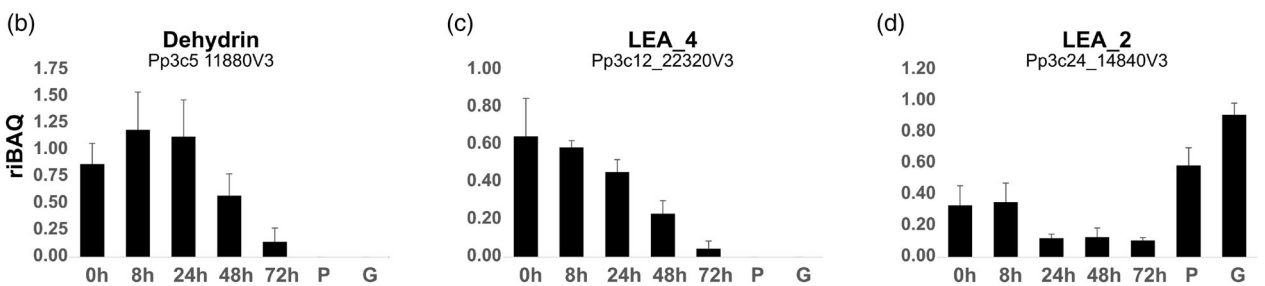

Figure 5. Most LEA proteins are enriched in early stages of spore germination (a) Late embryogenesis abundant (LEA) proteins identified in *Physcomitrium patens* clustered as visualized in Figure 1(c). Given are averaged relative iBAQ values (in ‰ of total protein abundance) for all developmental stages (spores 0, 8, 24, 48, 72, protonema (P), gametophore (G); $n = 5$ for each stage), the cluster number, the identifier of *P. patens*, the identifier of the most similar Arabidopsis homolog as well as the protein family. (b–d) Relative protein distribution of three selected LEA proteins. Error bars, SD.

More specifically, we identified two sub-clades of mitochondrial- and/or plastidial-targeted LEAs, and a distinct clade that was more associated with secretory pathway targeting (Figure 6). As two of these sub-clades contain proteins from both Arabidopsis and *P. patens*, it can be speculated that the subcellular targeting has been evolutionarily conserved at least since bryophytes and vascular plants diverged.

The other LEA families appeared at different times during the evolution of the green lineage, with LEA_2 and seed maturation protein (SMP) having emerged in the last common ancestor (LCA) of streptophytes and LEA_1 and dehydrins in the LCA of embryophytes (Figure S2).

LEA_6 and LEA_3 families are exclusive to spermatophytes (Figure S2); both families are mostly associated with seed- and/or pollen stages (Figure 6). Yet, seed- and pollen-associated LEA proteins are also found across other LEA families, often sharing homologs with the bryophyte *P. patens* (Figure 6). Moreover, the angiosperm-specific LEA_3 family stands out for having members from rice and Arabidopsis, which were all predicted and partially confirmed to be targeted to mitochondria (Figure S2). Lastly, the LEA_2 clade can be split into two sub-clades, with one of them being the only clear sub-clade of LEA proteins, which is predominantly associated with the vegetative stages (Figure 6).

Lipid droplet proteins and their role during ripening and germination of spores and seeds

One hallmark of seeds and other desiccated structures is the occurrence of a large number of lipid droplets that store neutral lipids, such as triacylglycerol (Guzha et al., 2023). However, these structures also occur in non-desiccated tissues and their function might be reflected by their proteomes (Ischebeck et al., 2020). While we did not isolate LDs in this study, 15 homologs to known LD proteins were found in the dataset, allowing us to study their developmental pattern (Figure 7; Data S13). In total, LDs made up 11.9% of all proteins in the spores, which was much higher than in protonema (0.05%) and gametophore (0.4%) tissues and even higher than in Arabidopsis seeds (5.7%; Kretzschmar et al., 2020).

The most abundant putative LD protein in *P. patens* spores is a homolog of OIL BODY LIPASE 1 (Figure 7, OBL1, Pp3c3_4690V3.2). The homologous protein is primarily found in developing and mature seeds of Arabidopsis (Klepikova et al., 2016), as well as in emerging pollen tubes of Arabidopsis and *Nicotiana tabacum*, potentially supplying TAG-derived membrane lipids there (Müller & Ischebeck, 2018). During spore germination, its abundance decreases by approximately 88.7% within 72 h and is nearly depleted in the protonema and gametophore stages. In addition to this dominant isoform, three additional homologs were identified. The second most abundant family of proteins in the spores were oleosins that are the main LD proteins in most seeds (Guzha et al., 2023). Furthermore, homologs to the other two most abundant proteins in seeds, caleosins, and steroleosins, were found almost exclusively in spores. Steroleosins are thought to be important for the metabolism of brassinosteroids (Lin et al., 2002), while caleosins might have a peroxygenase activity (Hanano et al., 2023) and are considered to play a role in stress-related processes (Aubert et al., 2010; Shimada et al., 2014). The LIPID DROPLET-ASSOCIATED PROTEIN 3 (LDAP3, Pp3c19_21240V3.2) and its interaction partner LDAP-INTERACTING PROTEIN (LDIP, Pp3c25_6290V3.3) are also predominantly found in spores. However, LDAP remains at a constant level, whereas LDIP decreases during germination. While these proteins are needed for the proper formation of LDs (Pyc et al., 2021), LDAP might have an additional coating function and is found also in vegetative tissues (Brocard et al., 2017; Gidda et al., 2016). Other proteins were not predominantly found in spores. One example is PLANT UBX DOMAIN-CONTAINING PROTEIN 10 (PUX10) that is involved in the degradation of ubiquitinated LD-associated proteins in Arabidopsis (Deruyffelaere et al., 2018; Kretzschmar et al., 2018) and that we found in similar amounts in all analyzed stages. The two proteins involved in sterol metabolism a putative cycloartenol synthase and sterol methyl transferase 1 showed the highest levels in the late stages of spore germination and vegetative tissues, respectively.

A bimodal expression pattern of lipoxygenases in *P. patens*

The share of lipoxygenases and allene oxide synthases was comparably high in 0 h spores, making up 9.6% of all proteins, dropping to 2.4% in 72 h spores. The levels in protonemata (0.37%) and gametophores (0.33%) were much lower (Data S14), implying a pivotal role during spore germination. Consistently, *Pp*LOX4b (Pp3c14_10640V3.1) is the second most abundant protein in 0 h spores (Data S2). LOX proteins oxygenate polyunsaturated fatty acids, which can be metabolized to oxylipins, volatiles, or designate the oxygenated fatty acid for degradation (Andreou & Feussner, 2009). Furthermore, specific isoforms were observed as LD-associated proteins in some species (Feußner & Kindl, 1992). The different types of plant LOXs can be classified based on their targeting signals for either plastidial or non-plastidial LOX, as well as their specificity for the oxygenation of α-linoleic acid (Andreou & Feussner, 2009). Our proteomic dataset identified seven LOX proteins and two AOS proteins (Data S14). LOX proteins and their enzymatic activity were annotated according to (Anterola et al., 2009). Pp3c1_29700V3.2.p, with the highest similarity to PpLOX6, was named by us PpLOX10. Then, the consensus of putative subcellular targeting was determined by assessing three distinct localization prediction tools (Figure 8).

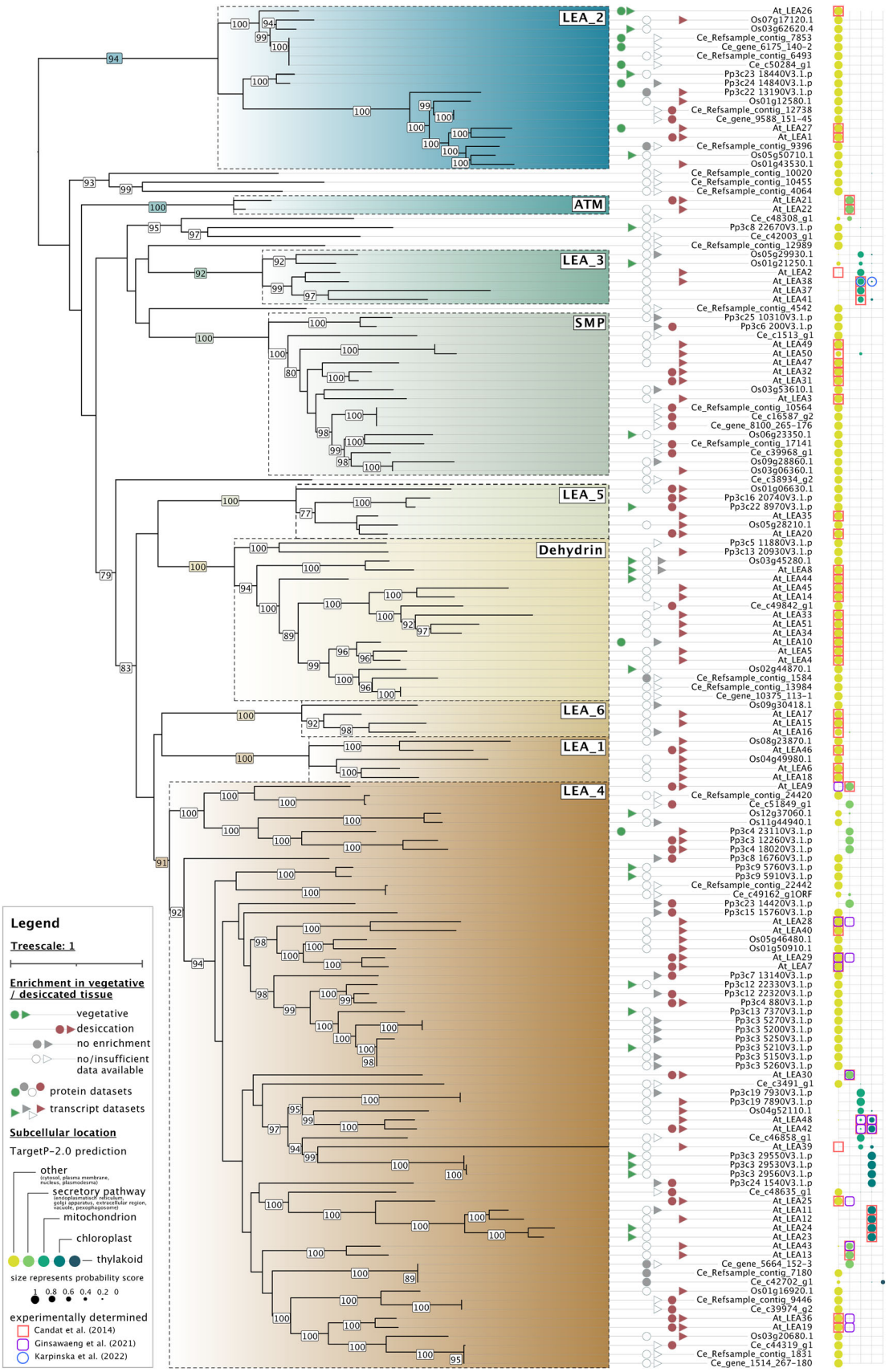

Figure 6. Phylogenetic tree of LEA proteins of *P. patens* and three Angiosperms. Phylogeny of LEA proteins including information on their expression and subcellular location. The tree was constructed with LEA proteins from 23 different Viridiplantae species and pruned for the LEAs of Arabidopsis (At) and their homologs found in *C. esculentus* (Ce), *O. sativa* (Os), and *P. patens* (Pp). Localizations were predicted with TargetP or are based on experimental data Ginsawaeng et al., 2021). Assignment as desiccation or vegetative enriched (>2-fold) is based on previously published data. See Experimental Procedures for details.

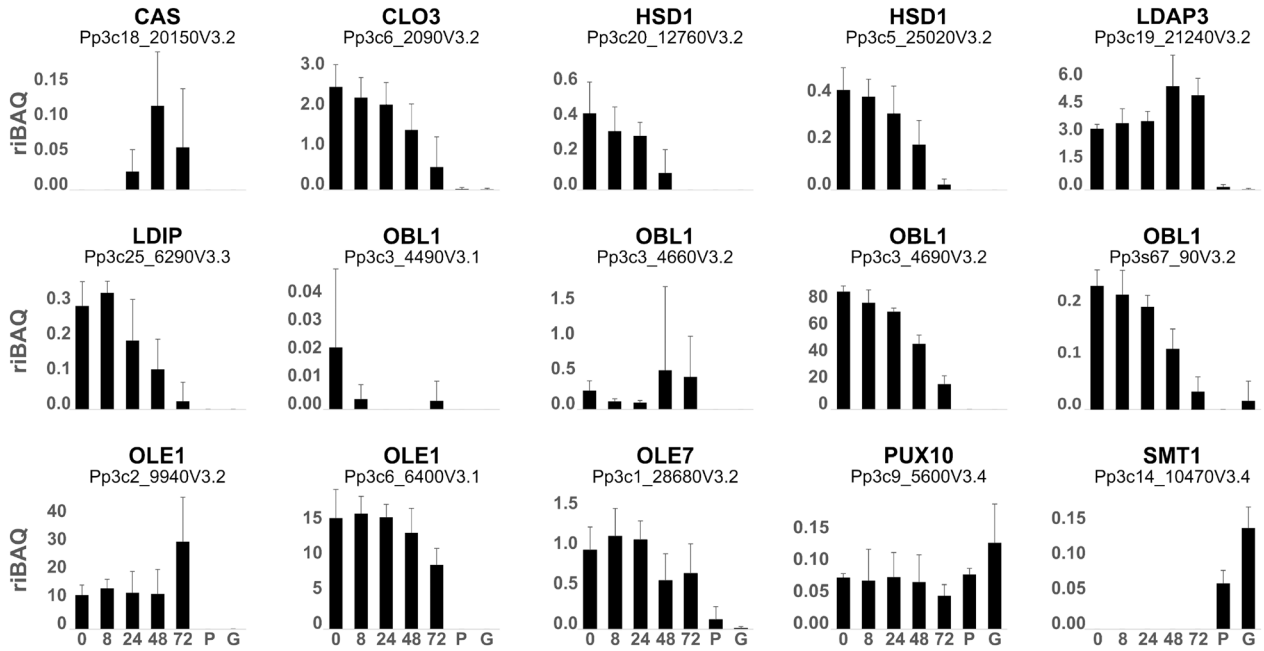

Figure 7. Most LD proteins are predominantly found in spores. Abundance of protein homologs of known LD proteins (spores 0, 8, 24, 48, 72 h; P, protonema; G, gametophore). *n* = 5 for each tissue. Error bars, SD. CAS, cycloartenolsynthase; CLO, caleosin; HSD, hydroxysteroid dehydrogenase, steroleosin; LDAP, lipid droplet-associated proteins; LDIP, LDAP-interacting protein; OBL, oil body lipase; OLE, oleosin; PUX, plant UBX domain-containing protein; SMT, sterol methyl transferase.

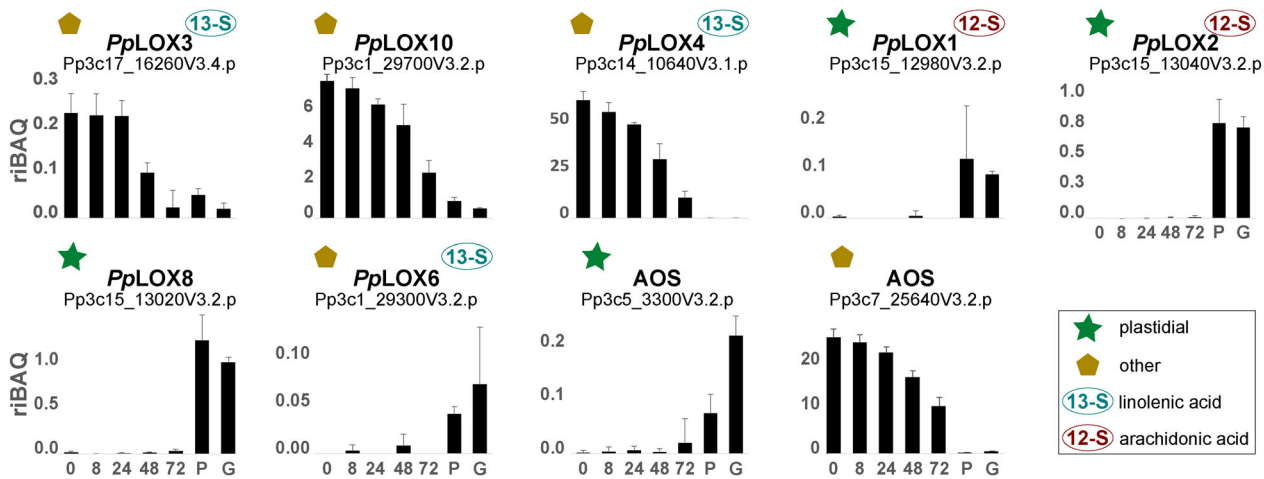

Figure 8. LOX pathway-related proteins in *P. patens*. Abundance of protein homologs of LOX pathway-related proteins (spores 0, 8, 24, 48, 72 h; P, protonema; G, gametophore). *n* = 5 for each tissue. Error bars, SD. Subcellular localization was predicted using the software tools LOCALIZER, Green Targeting Predictor, and TargetP 2.0, and a consensus is given. The substrate specificity and the position of the oxygen addition was annotated according to Anterola et al. (2009).

The protein abundance of LOX pathway-related genes shows a bimodal pattern. The first pattern is a high abundance in the vegetative stages with much lower levels in germinating spores. This trend is particularly evident in those LOX and AOS enzymes, which are predicted to be localized within the plastids and exhibit 12-S substrate specificity to arachidonic acid. The second pattern is observed in LOX and AOS enzymes, which are predicted to

be non-plastidial in their localization and exhibit 13-S substrate specificity to α-linolenic acid. These enzymes are primarily expressed in spores, and a general trend of decreasing relative abundance is observed during germination.

DISCUSSION

Both spore and seed germination, and seedling establishment progress through similar key phases

Desiccation-tolerant spores and seeds are the prime reproductive dispersal units of mosses and seed plants, respectively, and hallmarks of plant evolution. While they can be considered analogous structures, due to their expression in different generations, they share many similarities not only in their function but also on the molecular level (Pacini, 2012). Furthermore, the similarities are not restricted to the desiccated stage but extend to the establishment of a photoautotrophic plant from the heterotrophic energy-rich spore or seed. Both seeds and spores undergo four key phases that partially overlap. The first phase is defined by desiccation tolerance and already comprises the late phase of spore and embryo development. In the second phase, the cells are rehydrated and metabolism is activated. Furthermore, it is determined if the spore or seed germinates or remains dormant. The third phase is characterized by the degradation of TAG and the activation of β-oxidation and the glyoxylate cycle to generate energy and carbohydrates for cellular growth. During the fourth phase, the photosynthetic apparatus is established, leading to full photoautotrophy. We will discuss the individual phases in the context of similarities and differences between Arabidopsis and *P. patens*.

Phase 1 several protein families mediate desiccation tolerance

LEAs proteins play a key role in protecting proteins and membranes in desiccated structures of all eukaryotes including spores, pollen and seeds of plants (Chakrabortee et al., 2012; Grelet et al., 2005; Hibshman & Goldstein, 2021; Hundertmark et al., 2011; Li et al., 2012; Tolleter et al., 2010). They are also strongly upregulated in resurrection plants during desiccation (Gechev et al., 2021). Evolutionary oldest according to our analysis are the LEA_4 and LEA_5 families. In line with this, they have been found in many animal species as well. For example, rotifers, nematodes and tardigrades possess LEA_4 homologs and a LEA_5 protein was identified in the brine shrimp *Artemia franciscana* (Hand et al., 2011), where they likely have a desiccation related function as well. According to this function, most of these proteins are largely degraded within 72 h in *P. patens* spores and also after 36 h in seedlings (Kretzschmar et al., 2020) and 5 h in pollen tubes (Data S6). An exception are two LEA_2 and several LEA_4 proteins that were found predominantly in vegetative tissues of *P. patens* based on proteomic and transcript data (Figures 5 and 6). Interestingly the LEA_2 proteins are closely related to LEA proteins of seed plants that are also predominantly found in non-desiccated organs (Figure 6). Also, the organelle targeting of certain LEA proteins seems to be conserved between mosses and seed plants as members of a sub-clade of the LEA_4 family have been shown (Ginsawaeng et al., 2021) or are predicted to target plastids and mitochondria (Figure 6).

Throughout plant evolution, the number of LEA protein families has increased in plants (Figure S2), with LEA_1, LEA_3, and LEA_6 not being present in *P. patens*. The members of the LEA_1 and LEA_6 families are all found in desiccated structures (Artur et al., 2019), while the LEA_3 family have all been shown or predicted to target mitochondria indicating a specialized function for these LEA clades. Interestingly dehydrin-type LEA proteins are found in *P. patens* but have not been recorded in streptophyte algae. They could have evolved in the early land plants and helped to cope with the specific stresses encountered on land.

Both spores of *P. patens* and Arabidopsis seeds contain a large number of LDs and also these structures have to be protected to prevent them from fusing. Oleosin-coding genes increase upon environmental stress in extant representatives of the closest algal lineage to land plants, the Zygnematophyceae (Dadras et al., 2023; de Vries et al., 2020), and oleosin proteins are enriched in the LD proteomes of the zygnematophyte alga *Mesotaenium endlicherianum* (Dadras et al., 2023); it is thus likely that they were part of the toolbox for environmental responses in the earliest land plants. Indeed, the high number of lipid droplets in the durable and resilient zygospores (Permann et al., 2023) as well as the pre-akinetes (Pichrtová et al., 2016) of zygnematophytes like *Zygnema* suggests that such a toolkit for endurance was present in the last common ancestor of zygnematophytes and land plants. Oleosins are commonly found in desiccated tissues, including spores, pollen, and seeds (Guzha et al., 2023). Their importance during desiccation is corroborated by the diminished or deficient presence of oleosins in desiccation-sensitive (recalcitrant) seeds (Leprince et al., 1997) and by the heightened susceptibility to freezing of oleosin-reduced Arabidopsis seeds (Shimada et al., 2008). Conversely, augmented levels of oleosins were observed in desiccated vegetative tissues of resurrection plants on the transcript level (Costa et al., 2017; VanBuren et al., 2017; Xu et al., 2018) and in the proteome of the desiccation-tolerant tubers of *C. esculentus* (Niemeyer et al., 2022; Yang et al., 2016). In *P. patens*, oleosins might also be present in vegetative tissues. While transcript levels are very low under control conditions two oleosins increase more than 100-fold after 24 h of ABA treatment of

protonemata reaching 4–7% of the levels in spores (Data S13b; Perroud et al., 2018). These oleosins could coat LDs in brood cells that are formed after ABA treatment and contain many LDs as shown for several moss species (Goode et al., 1994; Rowntree et al., 2007; Schnepf & Reinhard, 1997).

Another prominent LD-associated protein family in both spores and seeds are the caleosins (Figure 7; Guzha et al., 2023). In Arabidopsis, CLO1 and 2 are highest in seeds (Kretzschmar et al., 2020), CLO3 in leaves (Fernández-Santos et al., 2020), and CLO4 in pollen (Ischebeck, 2016). Such an organ-specific expression also seems to be the case in *P. patens*, with one gene (Pp3c6_2090V3) being highest expressed in spores, while the other two isoforms are strongly upregulated under ABA treatment and dehydration in vegetative tissues (Data S13b; Fernandez-Pozo et al., 2020; Perroud et al., 2018).

Phase 2 spore and seed germination are regulated by similar factors

In Arabidopsis seeds, it was shown that metabolism is initiated very quickly during rehydration, with ATP being produced within minutes (Nietzel et al., 2020). While a similar study has not been performed for *P. patens* spore germination, all the proteins required for energy generation are readily available, with the GO term "glycolytic process" being highest in dry spores and then slowly decreasing (Figure 2), and subunits of the mitochondrial ATP synthase complex also being present (Data S2b).

By activating their metabolism, spores, and seeds take the first steps required for germination. However, germination can also be suppressed by a complex regulatory network leading to spores and seeds staying dormant (Nonogaki, 2014; Vesty et al., 2016). Part of this regulatory network are hormones, including ABA and, at least in seeds, brassinosteroids.

While *P. patens* spores do not seem to have a primary dormancy, their germination can be suppressed, for example, by ABA similar to seeds (Moody et al., 2016; Sano & Marion-Poll, 2021; Vesty et al., 2016). ABA might also be involved in the accumulation of certain proteins during spore maturation, as many of the proteins found in dry spores have homologs to ABA-responsive proteins in Arabidopsis. Furthermore, we detected an AWPM-19-like membrane family protein in both spores (Data S11c) and Arabidopsis seeds (Kretzschmar et al., 2020) that might be involved in ABA transport and thereby ABA signaling based on the function of a homolog in rice (Yao et al., 2018).

Brassinosteroids are plant hormones involved in growth and developmental processes (Clouse & Sasse, 1998; Peres et al., 2019) that also occur in moss with a proposed function in development (Morikawa et al., 2009; Yokota et al., 2017). Brassinosteroids impact spore germination in ferns (Gómez-Garay et al., 2018) and in seeds of Arabidopsis (Leubner-Metzger, 2003) and rice (Xiong et al., 2022). It remains uncertain whether this effect applies to bryophyte spores. Steroleosins are major LD proteins in Arabidopsis seeds (Kretzschmar et al., 2020) and also abundant in *P. patens* spores (Figure 7), but are not found in drought-stressed leaves (Doner et al., 2021), indicating that they might not have a role in drought and desiccation responses but rather developmental processes. In line with this is a potential involvement in brassinosteroid metabolism by acting as dehydrogenases (Baud et al., 2009; Li et al., 2007), although the exact nature of their involvement is currently uncertain.

Another factor that influences dormancy is light perceived by specific receptors. In seeds of Arabidopsis, red light induces seed germination, while far-red light inhibits it (Jiang et al., 2016). Involved in this process is the phytochrome B photoreceptor HYPOCOTYL3 (HY3) that induces seed germination when perceiving red light but is inhibited by far-red light. A homolog of HY3 that we detected in dry spores (Data S3) was rapidly degraded within 48 h. Based on this finding, it could play an analogous role, especially since it was shown that *P. patens* spore germination is inhibited by far-red light as well (Vesty et al., 2016). Recently, it was found that a ortholog of the Arabidopsis DELAY OF GERMINATION 1 (Bentsink et al., 2006) alongside DELLA proteins regulates spore germination in *P. patens* highlighting another protein network important for both spore and seed germination (Vollmeister et al., 2023).

Phase 3 heterotrophic degradation of oil

With its high energy and carbon density, TAG is an optimal storage reserve. However, both spore germination and seedling establishment require mostly sugars for cell wall synthesis needed for cell expansion (Ischebeck et al., 2020). For this, the fatty acids derived from the TAG are degraded first by β-oxidation, and the resulting acetyl-CoA is converted to sugars by the glyoxylate cycle and gluconeogenesis. In Arabidopsis, there is a sharp increase in the abundance of proteins involved in β-oxidation and the glyoxylate cycle during the first 36 h and a decrease thereafter (Figure 2). In *P. patens* the levels of these enzymes are already much higher in dry spores, slightly increase during spore germination, and are still high after 72 h. In vegetative tissues, the levels are then much lower. The result suggest that *P. patens* spores, like Arabidopsis seedlings, utilize a large amount of TAG for sugar production but that this process takes longer. *N. tabacum* pollen tubes contain almost no proteins associated with the glyoxylate cycle (Figure 2), probably because they can take up sugars from the carpel tissue. Therefore, the degradation of fatty acids might be utilized for energy generation instead.

By contrast, the way the fatty acids are released from TAG might be different in each species. In Arabidopsis, the majority of TAG is hydrolyzed by the lipase

SUGAR-DEPENDENT 1 (SDP1) and its homolog (Kelly et al., 2011), while the knockout of the major oil body lipase (OBL)-type TAG lipase does not affect TAG breakdown during seed germination (Müller & Ischebeck, 2018). The physiological function of this protein family is, therefore, mostly unclear in Arabidopsis, but a homolog in tomato (*Solanum lycopersicum*) is involved in the production of oxylipin-derived volatiles (Garbowicz et al., 2018; Ischebeck et al., 2020).

The genome of *P. patens* codes for four homologs of SDP1, but none of these were found in our proteomic dataset (Data S2) and their expression levels are also more than 100 times lower than for the lipases of the OBL family (Fernandez-Pozo et al., 2020). Furthermore, based on this study, the OBL Pp3c3_4690V3 is the most abundant protein indicating a pivotal role in TAG degradation (Data S2b). Based on the findings of Garbowicz et al., a plausible function of OBLs in germinating spores is the liberation of LOX-oxygenated fatty acids, especially considering that a putative cytosolic 13-S LOX was found to be the second most abundant protein (Data S2b). Interestingly, there is also evidence pointing towards a catabolic role of at least the LOX genes in cucumber seedlings and olive pollen tubes (Feussner et al., 1997, 2001; Matsui et al., 1999; Zienkiewicz et al., 2013). In the present case, an analogous process could apply, using a 13-S LOX enzyme to first generate a 13S-hydroperoxide-octadecadienoic acid (13-HPODE) from linoleic acid, which gets then reduced to 13S-hydroxy-octadecadienoic acid (13-HODE) and released to the cytosol and glyoxysomes for ß-oxidation. The cucumber 13-LOX was described as LD-associated in cotyledons (Feußner & Kindl, 1992; Hause et al., 2000), and LD-associated LOX were also observed in cotyledons and pollen tubes of olive (Zienkiewicz et al., 2013, 2014), and sunflower seeds (Yadav & Bhatla, 2011). Similarly, the main *P. patens* LOX could be associated with LDs and drive TAG breakdown in combination with the OBLs. It is so far not clear if TAG could be degraded by a similar mechanism in desiccation-resistant vegetative tissues after rehydration. ABA treatment induces the expression of the main spore LOX by 29-fold (Data S14b; Perroud et al., 2018) but the levels are still more than 5000-fold lower than in spores and no OBL coding genes were upregulated. In the resurrection grass *Oropetium thomaeum*, LDs accumulated during desiccation are mostly degraded within 2 days after rewatering (VanBuren et al., 2017) but it is not clear how the oil is degraded and how it is utilized.

In the zygnematophyte *Mesotaenium endlicherianum* high light and high temperature triggered a three-fold increase in the expression of the OBL homolog Me1_v2_0120870 (Dadras et al., 2023). In *N. tabacum* pollen tubes, two OBL homologs were found enriched on LDs (Kretzschmar, 2018) and they also play a role in pollen tube growth in *N. tabacum* and the homolog OBL1 in Arabidopsis (Müller & Ischebeck, 2018).

Phase 4 establishment of the photosynthetic apparatus

The constitution of the photosynthetic apparatus requires three main components: (i) the proteins and enzymes involved in the light and the dark reactions, (ii) the pigments of the light-harvesting complexes, and (iii) the membrane lipids of the thylakoids. All these components are missing or are strongly reduced in Arabidopsis seeds (Kehelpannala et al., 2021; Kretzschmar et al., 2020; Li et al., 2017), likely in part because desiccation increases the production of reactive oxygen species during the light reaction (Oliver et al., 2020). Proteins required for the light reaction and the Calvin cycle are almost absent in dry seeds and start to strongly increase 24 h after imbibition, with the increase maybe not being completed after 72 h (Figure 2). In *P. patens*, the levels in spores are already a little bit higher, and start to increase after 24 h, but are still much lower after 72 h than in protonema and gametophore tissues indicating that the build-up is far from being completed. The increase in Arabidopsis goes in hand with degradation of storage proteins that could deliver amino acids for this purpose. *P. patens* does not have obvious storage proteins, but the degradation of for example the most abundant proteins OBL and LOX (Figures 7 and 8) could provide amino acids for the synthesis of photosynthesis-related proteins.

Proteins involved in chlorophyll synthesis start to increase after 24 h in both Arabidopsis and *P. patens* and continuously increase (Figure 2). In Arabidopsis, a similar trend is observed for proteins involved in fatty acid synthesis. Interestingly, this is not the case in *P. patens*, where fatty acid synthesis is highest in spores and then decreases with the levels. This difference indicates that Arabidopsis synthesizes most of the fatty acids required for membrane lipid synthesis *de novo*, while *P. patens* might make use of fatty acids derived from TAG breakdown.

EXPERIMENTAL PROCEDURES

Plant material

Physcomitrium patens of the ecotype Reute was grown as previously described (Gömann et al., 2021). Protonemata cultivated on BCDAT medium were harvested 8 days after propagation, and full-grown gametophores cultivated on BCD medium 35 days after propagation. Sporophytes were induced as previously described (Hiss et al., 2017) and individually picked. Spore capusles were transferred into ddH_2O and broken up in a reaction cup using a mini plastic mortar before being distributed to 24 well plates containing 1 ml ddH_2O each. Spores and some of the spore capsule debris were harvested after 15 min (0 h), 8, 24, 48, and 72 h by spinning down the spores at 2000 ***g*** for 10 sec and removing the water. After harvesting, the material was flash-frozen in liquid nitrogen and stored at −80°C.

Isolation of protein fractions from moss

Frozen spores or germinated spores including some spore capsule remnants (derived from 2.5 mg spore capsules per sample) were ground in a liquid nitrogen-cooled shaking mill (Retsch, Haan, Germany) with three 2.5 mm steel beads at 30 Hz for 2 min. Subsequently, 30–50 µl protein solubilization buffer (6 M Urea, 5% SDS, 2 mM phenylmethylsulfonyl fluoride) was added, followed by flash freezing in liquid nitrogen. Protonema and gametophore material was ground in a liquid nitrogen-cooled mortar. Following, 40 mg material was added into 100 µl protein solubilization buffer and thawed on ice before flash freezing in liquid nitrogen again. All samples were then treated in an ice-cooled ultrasonic bath for 15 min and centrifuged at 4°C for 10 min at 19.000 ***g***. The supernatant was collected and used for further processing.

Preparation of peptide samples and LC–MS/MS

All proteomic metadata can be found in Table S1. For the determination of protein concentration, the Pierce BCA protein assay kit (Thermo Fisher Scientific, Waltham, MA, USA) was used according to the manufacturer's instructions. In the following, 20 µg (germinating spores) or 30 µg (protonema/gametophores) of protein per replicate were subjected to electrophoresis on an SDS-acrylamide gel, with the run being halted once the proteins had entered the separation gel by approximately 3–5 mm. Individually excised gel pieces were processed and tryptically digested as previously described (Shevchenko et al., 2006). Subsequently, the resulting peptides were desalted via a custom EmporeTM Octadecyl C18 47 mm extraction disks 2215 (Supelco, St. Paul, MN, USA) filled columns as described elsewhere (Rappsilber et al., 2007). Purified peptides were suspended in 20 µl LC–MS sample buffer (2% acetonitrile, 0.1% formic acid) prior to applying it to reverse phase LC-based peptide separation on an RSLCnano Ultimate 3000 system (Thermo Fisher Scientific). Peptides were loaded with 0.07% trifluoroacetic acid onto a C18 Acclaim PepMap 100 precolumn (100 µm × 2 cm, 5 µm particle size, 100 Å pore size; Thermo Fisher Scientific) set to a flow rate of 20 µl min^{-1} for 3 min. The peptides were then separated analytically using a C18 Acclaim PepMap RSLC column (75 µm × 50 cm, 2 µm particle size, 100 Å pore size; Thermo Fisher Scientific) at a flow rate of 300 nl min^{-1}. The solvent composition underwent a gradient change, initiating at 96% solvent A containing 0.1% formic acid and 4% solvent B consisting of 80% acetonitrile and 0.1% formic acid. Over a period of 94 min, the proportion of solvent B increased progressively to 10% within 2 min, followed by a further increase to 30% within the subsequent 58 min. This was followed by an additional rise to 45% solvent B within the following 22 min, culminating in a peak of 90% solvent B in the last 12 min of the gradient. Optima-grade (Thermo Fisher Scientific) solvents and acids were used for all LC–MS experiments. Eluting peptides were ionized online by nano-electrospray (nESI) using a Nanospray Flex Ion Source (Thermo Fisher Scientific) at 1.5 kV (liquid junction) and transferred to a Q Exactive HF mass spectrometer (Thermo Fisher Scientific). Full scans were recorded in a mass range of 300–1650 m/z at a resolution of 30 000, followed by data-dependent top 10 HCD fragmentation at a resolution of 15 000 (dynamic exclusion enabled). XCalibur 4.0 software (Thermo Fisher Scientific) was used for the LC–MS method programming and data acquisition.

Proteomic RAW data processing

Proteomic RAW data were processed in MaxQuant 2.0.3.1 software (Cox & Mann, 2008; Tyanova, Temu, & Cox, 2016) on default settings except enabling "Label-free quantification - LFQ," "iBAQ," "FTMS recalibration," "Match between runs," and set "Intensity determination" to "Total sum." The *P. patens* primary transcript protein file (v3.3, DOE-JGI; https://phytozome-next.jgi.doe.gov/; Goodstein et al., 2012; Lang et al., 2018) was used as reference library. Filtering and relative iBAQ (riBAQ) normalization (‰ of total protein abundance per sample) from the resulting MaxQuant proteinGroups file was performed in Perseus 1.6.2.2 (Tyanova, Temu, Sinitcyn, et al., 2016) as previously described (Horn et al., 2021). The raw data on the *N. tabacum* pollen proteome (Ischebeck et al., 2014) was reprocessed with MaxQuant using the same settings and the database based on the *N. tabacum* genome (Edwards et al., 2017).

Blast

In order to identify the closest homologs of *P. patens* proteins in Arabidopsis, a BLASTp approach was employed (Altschul et al., 1990; Gish & States, 1993). Here, the *P. patens* primary transcript protein file (v3.3, DOE-JGI; https://phytozome-next.jgi.doe.gov/; Goodstein et al., 2012; Lang et al., 2018) was used as a query against the Arabidopsis TAIR10 primary transcript protein release (Lamesch et al., 2012). BLAST software release 2.11.0+ was used, and an E-value cutoff of $<10^{-5}$ was set.

Data analysis

PCA plots, hierarchical clusters, and volcano plots were created with Perseus 1.6.2.2 (Tyanova, Temu, Sinitcyn, et al., 2016). The PCA was created using standard settings. The hierarchical clustering was performed based on Euclidean distance for row clusters, and Euclidean (Figure 1) or Pearson distance (Figure 3) for column clusters. Data was preprocessed with k-means, and the number of iterations was set to 10 with 100 restarts. For the volcano plots, data were imputed with a width of 0.3 and a downshift of 1.8. Significance was assessed via *t*-test, setting the number of randomizations to 250, the false discovery rate to 0.05, and the S_0 to 0.1.

For GO term analysis, all *P. patens* accessions were assigned an Arabidopsis accession based on homology determined by the BLAST search (lowest *E*-value). When several *P. patens* were assigned to the same Arabidopsis protein, their riBAQ values were added. Then, these values were assigned to each AGI-accession GO term pair (retrieved from www.arabidopsis.org September 1, 2022), and the protein abundance in each GO term was determined by adding the riBAQ of all the proteins therein.

Phylogenetic analysis of LEA proteins

To identify homologs of LEA proteins, the previously identified LEA proteins from *A. thaliana* (Hundertmark & Hincha, 2008) were used as a query in a BLASTp against a protein database with an *E*-value cutoff $<10^{-5}$. The database of (predicted) proteins was assembled from the genomes of *Anthoceros agrestis* (Li et al., 2020), *Amborella trichopoda* (AMBORELLA GENOME PROJECT et al., 2013) *A. thaliana* (Lamesch et al., 2012), *Azolla filiculoides* (Li et al., 2018), *Brachypodium distachyon* (Vogel et al., 2010), *Chlorokybus melkonianii* (Irisarri et al., 2021; Wang et al., 2020), *Chara braunii* (Nishiyama et al., 2018), *Chlaymdomonas reinhardtii* (Merchant et al., 2007), *Coccomyxa subellipsoidea* (Blanc et al., 2012), *Ceratopteris richardii* (Marchant et al., 2022), *C. esculentus* (Niemeyer et al., 2022; Yang et al., 2016), *Gnetum montanum* (Wan et al., 2018), *Isoetes taiwanensis* (Wickell et al., 2021), *Klebsormidium nitens* (Hori et al., 2014), *Marchantia polymorpha* (Bowman et al., 2017), *Mesotaenium endlicherianum* (Cheng et al., 2019; Dadras et al., 2023), *O. sativa* (Ouyang et al., 2007), *Picea abies* (Nystedt et al., 2013), *Penium margaritaceum* (Jiao et al., 2020), *P. patens* (Lang et al., 2018), *Selaginella*

moellendorffii (Banks et al., 2011), *Spirogloea muscicola* (Cheng et al., 2019), and *Ulva mutabilis* (De Clerck et al., 2018). Sequences (Data S15) were aligned with MAFFT (Katoh & Standley, 2013) using the alignment method L-INS-i. The maximum-likelihood tree was constructed with IQ-Tree (Minh et al., 2020) in which the WAG+I + G4 model was selected as most suitable by ModelFinder (Kalyaanamoorthy et al., 2017) utilizing the option -madd LG4M,LG4X. The branch support was assessed with ultrafast bootstrap (Hoang et al., 2018). All data on the tree construction can be found in Data S16–S18. The visualization was done in iTOL version 2.0.3 (Letunic & Bork, 2007), and the given subcellular locations of the proteins were predicted with TargetP-2.0 (Armenteros et al., 2019).

Analysis of LEA expression data

LEA mRNA transcripts from different RNAseq databases were retrieved for three species: TraVa for *Arabidopsis thaliana* ecotype Col-0 (Transcriptome Variation Analysis database; http://travadb.org/; Klepikova et al., 2016), RED for *O. sativa* cv. Nipponbare (Rice Expression Database; http://expression.ic4r.org/; (Xia et al., 2017), and PEATmoss for *Physcomitrium patens* ecotypes Gransden and Reute (https://peatmoss.plantcode.cup.uni-freiburg.de/; (Fernandez-Pozo et al., 2020). LEA protein data were acquired from *A. thaliana* ecotype Col-0 (Kretzschmar et al., 2020), *Cyperus esculentus* L. var. *sativus* (Niemeyer et al., 2022), and *P. patens* ecotype Reute (this publication).

Due to varying data availability, we chose different desiccation- and vegetative-associated stages for each species. For the Arabidopsis ecotype Col-0 transcripts, we compared seeds of the first yellowing silique, dry seeds, opened anthers, and anthers from mature unopened flowers with germinating seeds 3 days after imbibition, seedling cotyledons, seedling roots, and whole mature leaves; while for protein expression data, seeds 30 min after imbibition and seedlings 60 h after imbibition were chosen. For *P. patens* transcripts, both Gransden and Reute ecotypes were included; namely, we compared dry spores (Gransden) and brown sporophytes (Reute) against protonema (Gransden and Reute), gametophores (Gransden and Reute), adult gametophores (Reute) and leaflets (Gransden). For the protein analysis of *P. patens* ecotype Reute, dry spores were compared with gametophores and protonema. For *O. sativa* cv. Nipponbare transcripts, mature seeds and anthers from mature unopened flowers were contrasted to 14-day-old shoots, roots, and leaves. No protein expression data were analyzed for rice. Lastly, for *C. esculentum* L. var. *sativus* – for which only proteome data was used – dry tubers were compared to leaves and roots.

We determined the ratio between the highest raw value of the before-mentioned desiccation- and vegetative-associated stages. An LEA transcript or protein was considered desiccation or vegetative stage-specific when the ratio of the raw normalized mRNA levels, or riBAQ values were at least 2-times higher in desiccation-associated tissues compared to vegetative-associated tissues and *vice versa*.

Prediction of LOX subcellular targeting and substrate affinity

The annotation of *P. patens* LOX and AOS proteins is based on their closest homologs in Arabidopsis and was determined by a BLASTp search. The substrate specificity for the LOX proteins was assigned based on a previous characterization study (Anterola et al., 2009). The subcellular localization of the identified LOX and AOS proteins was predicted using three different computational tools, namely LOCALIZER (https://localizer.csiro.au/; Sperschneider et al., 2017), Green Targeting Predictor (https://plantcode.cup.uni-freiburg.de/plantco/predloc/; Fuss et al., 2013), and TargetP 2.0 (https://services.healthtech.dtu.dk/services/TargetP-2.0/; Armenteros et al., 2019). The consensus prediction from two out of three tools was considered as an indication of the subcellular localization of the LOX proteins.

AUTHOR CONTRIBUTIONS

LH, PWN, GHB, MS, JdV, SAR, and TI designed the work, LH, PWN, KS, JZ, DB, OV, JD, JdV, and TI performed research, LH, PWN, KS, PS, JdV, and TI analyzed data, and LH, PWN, JZ, DB, JD, and TI wrote the manuscript. All authors critically read and revised the manuscript and approved the final version.

ACKNOWLEDGMENTS

PWN, GB, JdV, and TI thank the German research foundation (DFG, Grants IS 273/7-1, IS 273/9-1, IS 273/10-1, IRTG 2172 PRoTECT, BR1502-15-1, VR 132/4-1); part of this work was conducted in the framework of MAdLand [http://madland.science; Deutsche Forschungsgemeinschaft (DFG) priority programme 2237], SAR is grateful for funding through RE 1697/19–1, 20–1), JdV thanks the European Research Council for funding (Grant Agreement No. 852725; ERC-StG "TerreStriAL") under the European Union's Horizon 2020 research and innovation program. OV and KS on behalf of the Service Unit LCMS Protein Analytics of the Göttingen Center for Molecular Biosciences (GZMB) thank the DFG for funding (INST 186/1230-1 FUGG to Stefanie Pöggeler). We thank Marco Göttig (University of Marburg) for extensive collection of spore capsules and Dr. Tegan Haslam and Ivo Feussner (University of Göttingen) for providing gametophores and protonemata. Open Access funding enabled and organized by Projekt DEAL.

CONFLICT OF INTEREST STATEMENT

The authors declare no conflict of interest.

SUPPORTING INFORMATION

Additional Supporting Information may be found in the online version of this article.

Figure S1. Pair-wise comparison of developmental stages through volcano plots.

Figure S2. Phylogenetic tree of LEA proteins in the green lineage.

Table S1. Proteomics meta data.

Data S1. Results of a BLASTp query of the *P. patens* proteins against the *Arabidopsis thaliana* TAIR10 primary transcript protein release.

Data S2. Normalized relative iBAQ values of *P. patens* proteins.

Data S3. Result of hierarchical clustering of *P. patens* proteins.

Data S4. GO term analysis.

Data S5. Results of a BLASTp query of the *N. tabacum* proteins against the *Arabidopsis thaliana* TAIR10 primary transcript protein release and the *P. patens* proteome.

Data S6. Normalized relative iBAQ values of *N. tabacum* proteins from pollen development.

Data S7. GO term analysis of *N. tabacum* proteins from pollen development.

Data S8. Normalized relative iBAQ values of *P. patens* and Arabidopsis proteins.

Data S9. Hierarchical clustering of the *P. patens* and Arabidopsis proteins.

Data S10. Normalized relative iBAQ values of *P. patens* and *N. tabacum* proteins and hierarchical clustering.

Data S11. Log_2 transformed and imputed data used for volcano plots.

Data S12. Overview of LEA proteins.

Data S13. Overview of LD proteins.

Data S14. Overview of LOX and AOS.

Data S15. Sequence alignment of LEA proteins.

Data S16. Lea tree file.

Data S17. Lea tree design Figure 6.

Data S18. Lea tree design Figure S2.

OPEN RESEARCH BADGES

This article has earned an Open Data badge for making publicly available the digitally-shareable data necessary to reproduce the reported results. The data is available at: all data can be found within the manuscript and its supporting materials. Proteomic raw data can be found in the PRIDE database (Vizcaíno et al., 2014) under the identifiers PXD043767 (*P. patens* data) and PXD045970 (*N. tabacum* data) (https://www.ebi.ac.uk/pride/).

DATA AVAILABILITY STATEMENT

All relevant data can be found within the manuscript and its supporting materials. Proteomic raw data can be found in the PRIDE database (Vizcaíno et al., 2014) under the identifiers PXD043767 (*P. patens* data) and PXD045970 (*N. tabacum* data; https://www.ebi.ac.uk/pride/).

REFERENCES

Altschul, S.F., Gish, W., Miller, W., Myers, E.W. & Lipman, D.J. (1990) Basic local alignment search tool. *Journal of Molecular Biology*, **215**, 403–410.

AMBORELLA GENOME PROJECT, Albert, V.A., Barbazuk, W.B., de Pamphilis, C.W., Der, J.P., Leebens-Mack, J. *et al.* (2013) The Amborella genome and the evolution of flowering plants. *Science*, **342**, 1241089.

Andreou, A. & Feussner, I. (2009) Lipoxygenases – structure and reaction mechanism. *Phytochemistry*, **70**, 1504–1510.

Anterola, A., Göbel, C., Hornung, E., Sellhorn, G., Feussner, I. & Grimes, H. (2009) Physcomitrella patens has lipoxygenases for both eicosanoid and octadecanoid pathways. *Phytochemistry*, **70**, 40–52.

Arif, M.A., Hiss, M., Tomek, M., Busch, H., Meyberg, R., Tintelnot, S. *et al.* (2019) ABA-induced vegetative diaspore formation in *Physcomitrella patens*. *Frontiers in Plant Science*, **10**, 315.

Armenteros, J.J.A., Salvatore, M., Emanuelsson, O., Winther, O., von Heijne, G., Elofsson, A. *et al.* (2019) Detecting sequence signals in targeting peptides using deep learning. *Life Science Alliance*, **2**, e201900429.

Arsovski, A.A., Popma, T.M., Haughn, G.W., Carpita, N.C., McCann, M.C. & Western, T.L. (2009) AtBXL1 encodes a bifunctional β-d-xylosidase/α-l-arabinofuranosidase required for pectic arabinan modification in Arabidopsis mucilage secretory cells. *Plant Physiology*, **150**, 1219–1234.

Artur, M.A.S., Zhao, T., Ligterink, W., Schranz, E. & Hilhorst, H.W.M. (2019) Dissecting the genomic diversification of late embryogenesis abundant (LEA) protein gene families in plants. *Genome Biology and Evolution*, **11**, 459–471.

Aubert, Y., Vile, D., Pervent, M., Aldon, D., Ranty, B., Simonneau, T. *et al.* (2010) RD20, a stress-inducible caleosin, participates in stomatal control, transpiration and drought tolerance in *Arabidopsis thaliana*. *Plant and Cell Physiology*, **51**, 1975–1987.

Banks, J.A., Nishiyama, T., Hasebe, M., Bowman, J.L., Gribskov, M., de Pamphilis, C. *et al.* (2011) The selaginella genome identifies genetic changes associated with the evolution of vascular plants. *Science*, **332**, 960–963.

Baud, S., Dichow, N.R., Kelemen, Z., d'Andréa, S., To, A., Berger, N. *et al.* (2009) Regulation of HSD1 in seeds of *Arabidopsis thaliana*. *Plant and Cell Physiology*, **50**, 1463–1478.

Bentsink, L., Jowett, J., Hanhart, C.J. & Koornneef, M. (2006) Cloning of DOG1, a quantitative trait locus controlling seed dormancy in Arabidopsis. *Proceedings of the National Academy of Sciences of the United States of America*, **103**, 17042–17047.

Berardini, T.Z., Mundodi, S., Reiser, L., Huala, E., Garcia-Hernandez, M., Zhang, P. *et al.* (2004) Functional annotation of the Arabidopsis genome using controlled vocabularies. *Plant Physiology*, **135**, 745–755.

Blanc, G., Agarkova, I., Grimwood, J., Kuo, A., Brueggeman, A., Dunigan, D.D. *et al.* (2012) The genome of the polar eukaryotic microalga *Coccomyxa subellipsoidea* reveals traits of cold adaptation. *Genome Biology*, **13**, R39.

Bowman, J.L., Kohchi, T., Yamato, K.T., Jenkins, J., Shu, S., Ishizaki, K. *et al.* (2017) Insights into land plant evolution garnered from the *Marchantia polymorpha* genome. *Cell*, **171**, 287–304.e15.

Brocard, L., Immel, F., Coulon, D., Esnay, N., Tuphile, K., Pascal, S. *et al.* (2017) Proteomic analysis of lipid droplets from Arabidopsis aging leaves brings new insight into their biogenesis and functions. *Frontiers in Plant Science*, **8**, 894.

Chakrabortee, S., Tripathi, R., Watson, M., Schierle, G.S., Kurniawan, D.P., Kaminski, C.F. *et al.* (2012) Intrinsically disordered proteins as molecular shields. *Molecular BioSystems*, **8**, 210–219.

Cheng, S., Xian, W., Fu, Y., Marin, B., Keller, J., Wu, T. *et al.* (2019) Genomes of subaerial Zygnematophyceae provide insights into land plant evolution. *Cell*, **179**, 1057–1067.e14.

Chi, Y.H., Koo, S.S., Oh, H.T., Lee, E.S., Park, J.H., Phan, K.A.T. *et al.* (2019) The physiological functions of universal stress proteins and their molecular mechanism to protect plants from environmental stresses. *Frontiers in Plant Science*, **10**, 750.

Cho, S.H., Hoang, Q.T., Kim, Y.Y., Shin, H.Y., Ok, S.H., Bae, J.M. *et al.* (2006) Proteome analysis of gametophores identified a metallothionein involved in various abiotic stress responses in *Physcomitrella patens*. *Plant Cell Reports*, **25**, 475–488.

Clouse, S.D. & Sasse, J.M. (1998) BRASSINOSTEROIDS: essential regulators of plant growth and development. *Annual Review of Plant Physiology and Plant Molecular Biology*, **49**, 427–451.

Costa, M.-C.D., Artur, M.A.S., Maia, J., Jonkheer, E., Derks, M.F.L., Nijveen, H. *et al.* (2017) A footprint of desiccation tolerance in the genome of *Xerophyta viscosa*. *Nature Plants*, **3**, 1–10.

Cove, D. (2005) The moss *Physcomitrella patens*. *Annual Review of Genetics*, **39**, 339–358.

Cox, J. & Mann, M. (2008) MaxQuant enables high peptide identification rates, individualized p.p.b.-range mass accuracies and proteome-wide protein quantification. *Nature Biotechnology*, **26**, 1367–1372.

Crowe, A.J., Abenes, M., Plant, A. & Moloney, M.M. (2000) The seed-specific transactivator, ABI3, induces oleosin gene expression. *Plant Science*, **151**, 171–181.

Cui, S., Hu, J., Guo, S., Wang, J., Cheng, Y., Dang, X. *et al.* (2012) Proteome analysis of *Physcomitrella patens* exposed to progressive dehydration and rehydration. *Journal of Experimental Botany*, **63**, 711–726.

Cuming, A.C. (2019) Evolution of ABA signaling pathways. In: Seo, Mitsunori & Marion-Poll, Annie (Eds.) *Advances in botanical research*. Amsterdam, The Netherlands: Elsevier, pp. 281–313.

Cuming, A.C., Cho, S.H., Kamisugi, Y., Graham, H. & Quatrano, R.S. (2007) Microarray analysis of transcriptional responses to abscisic acid and osmotic, salt, and drought stress in the moss, *Physcomitrella patens*. *New Phytologist*, **176**, 275–287.

Curien, G., Giustini, C., Montillet, J.-L., Mas-y-Mas, S., Cobessi, D., Ferrer, J.-L. *et al.* (2016) The chloroplast membrane associated ceQORH putative quinone oxidoreductase reduces long-chain, stress-related oxidized lipids. *Phytochemistry*, **122**, 45–55.

Dadras, A., Fürst-Jansen, J.M.R., Darienko, T., Krone, D., Scholz, P., Sun, S. *et al.* (2023) Environmental gradients reveal stress hubs pre-dating plant terrestrialization. *Nature Plants*, **9**, 1419–1438.

Daku, R.M., Rabbi, F., Buttigieg, J., Coulson, I.M., Horne, D., Martens, G. *et al.* (2016) PpASCL, the *Physcomitrella patens* anther-specific chalcone synthase-like enzyme implicated in sporopollenin biosynthesis, is

needed for integrity of the moss spore wall and spore viability. *PLoS One*, **11**, e0146817.

De Clerck, O., **Kao, S.-M.**, **Bogaert, K.A.** ***et al.*** (2018) Insights into the evolution of multicellularity from the sea lettuce genome. *Current Biology*, **28**, 2921–2933.e5.

de Vries, J., **de Vries, S.**, **Curtis, B.A.**, **Zhou, H.**, **Penny, S.**, **Feussner, K.** ***et al.*** (2020) Heat stress response in the closest algal relatives of land plants reveals conserved stress signaling circuits. *The Plant Journal*, **103**, 1025–1048.

de Vries, J. & **Ischebeck, T.** (2020) Ties between stress and lipid droplets pre-date seeds. *Trends in Plant Science*, **25**, 1203–1214.

Delahaie, J., **Hundertmark, M.**, **Bove, J.**, **Leprince, O.**, **Rogniaux, H.** & **Buitink, J.** (2013) LEA polypeptide profiling of recalcitrant and orthodox legume seeds reveals ABI3-regulated LEA protein abundance linked to desiccation tolerance. *Journal of Experimental Botany*, **64**, 4559–4573.

Deruyffelaere, C., **Purkrtova, Z.**, **Bouchez, I.**, **Collet, B.**, **Cacas, J.-L.**, **Chardot, T.** ***et al.*** (2018) PUX10 is a CDC48A adaptor protein that regulates the extraction of ubiquitinated oleosins from seed lipid droplets in Arabidopsis. *Plant Cell*, **30**, 2116–2136.

Doner, N.M., **Seay, D.**, **Mehling, M.**, **Sun, S.**, **Gidda, S.K.**, **Schmitt, K.** ***et al.*** (2021) *Arabidopsis thaliana* EARLY RESPONSIVE TO DEHYDRATION 7 localizes to lipid droplets via its senescence domain. *Frontiers in Plant Science*, **12**, 658961.

Edwards, K.D., **Fernandez-Pozo, N.**, **Drake-Stowe, K.**, **Humphry, M.**, **Evans, A.D.**, **Bombarely, A.** ***et al.*** (2017) A reference genome for *Nicotiana tabacum* enables map-based cloning of homeologous loci implicated in nitrogen utilization efficiency. *BMC Genomics*, **18**, 448.

Engel, P.P. (1968) The induction of biochemical and morphological mutants in the moss *Physcomitrella Patens*. *American Journal of Botany*, **55**, 438–446.

Farrant, J.M., **Lehner, A.**, **Cooper, K.** & **Wiswedel, S.** (2009) Desiccation tolerance in the vegetative tissues of the fern *Mohria caffrorum* is seasonally regulated. *The Plant Journal*, **57**, 65–79.

Fernandez-Pozo, N., **Haas, F.B.**, **Meyberg, R.**, **Ullrich, K.K.**, **Hiss, M.**, **Perroud, P.F.** ***et al.*** (2020) PEATmoss (Physcomitrella Expression Atlas Tool): a unified gene expression atlas for the model plant *Physcomitrella patens*. *The Plant Journal*, **102**, 165–177.

Fernández-Santos, R., **Izquierdo, Y.**, **López, A.**, **Muñiz, L.**, **Martínez, M.**, **Cascón, T.** ***et al.*** (2020) Protein profiles of lipid droplets during the hypersensitive defense response of Arabidopsis against *Pseudomonas* infection. *Plant and Cell Physiology*, **61**, 1144–1157.

Feussner, I., **Balkenhohl, T.J.**, **Porzel, A.**, **Kühn, H.** & **Wasternack, C.** (1997) Structural elucidation of oxygenated storage lipids in cucumber cotyledons: implication of lipid body lipoxygenase in lipid mobilization during germination. *Journal of Biological Chemistry*, **272**, 21635–21641.

Feussner, I. & **Kindl, H.** (1992) A lipoxygenase is the main lipid body protein in cucumber and soybean cotyledons during the stage of triglyceride mobilization. *FEBS Letters*, **298**, 223–225.

Feussner, I., **Kühn, H.** & **Wasternack, C.** (2001) Lipoxygenase-dependent degradation of storage lipids. *Trends in Plant Science*, **6**, 268–273.

Fuss, J., **Liegmann, O.**, **Krause, K.** & **Rensing, S.A.** (2013) Green targeting predictor and ambiguous targeting predictor 2: the pitfalls of plant protein targeting prediction and of transient protein expression in heterologous systems. *The New Phytologist*, **200**, 1022–1033.

Gaff, D.F. & **Oliver, M.** (2013) The evolution of desiccation tolerance in angiosperm plants: a rare yet common phenomenon. *Functional Plant Biology*, **40**, 315–328.

Garbowicz, K., **Liu, Z.**, **Alseekh, S.**, **Tieman, D.**, **Taylor, M.**, **Kuhalskaya, A.** ***et al.*** (2018) Quantitative trait loci analysis identifies a prominent gene involved in the production of fatty acid-derived flavor volatiles in tomato. *Molecular Plant*, **11**, 1147–1165.

Gechev, T., **Lyall, R.**, **Petrov, V.** & **Bartels, D.** (2021) Systems biology of resurrection plants. *Cellular and Molecular Life Sciences*, **78**, 6365–6394.

Gidda, S.K., **Park, S.**, **Pyc, M.**, **Yurchenko, O.**, **Cai, Y.**, **Wu, P.** ***et al.*** (2016) Lipid droplet-associated proteins (LDAPs) are required for the dynamic regulation of neutral lipid compartmentation in plant cells. *Plant Physiology*, **170**, 2052–2071.

Ginsawaeng, O., **Heise, C.**, **Sangwan, R.**, **Karcher, D.**, **Hernández-Sánchez, I.E.**, **Sampathkumar, A.** ***et al.*** (2021) Subcellular localization of seed-expressed LEA_4 proteins reveals liquid-liquid phase separation for LEA9 and for LEA48 homo- and LEA42-LEA48 heterodimers. *Biomolecules*, **11**, 1770.

Giraudat, J., **Hauge, B.M.**, **Valon, C.**, **Smalle, J.**, **Parcy, F.** & **Goodman, H.M.** (1992) Isolation of the Arabidopsis ABI3 gene by positional cloning. *The Plant Cell*, **4**, 1251–1261.

Gish, W. & **States, D.J.** (1993) Identification of protein coding regions by database similarity search. *Nature Genetics*, **3**, 266–272.

Gömann, J., **Herrfurth, C.**, **Zienkiewicz, K.**, **Haslam, T.M.** & **Feussner, I.** (2021) Sphingolipid Δ4-desaturation is an important metabolic step for glycosylceramide formation in *Physcomitrium patens*. *Journal of Experimental Botany*, **72**, 5569–5583.

Gómez-Garay, A., **Gabriel y Galán, J.M.**, **Cabezuelo, A.**, **Pintos, B.**, **Prada, C.** & **Martín, L.** (2018) Ecological significance of brassinosteroids in three temperate ferns. In: Fernández, H. (Ed.) *Current advances in fern research*. Cham: Springer International Publishing, pp. 453–466.

Gong, Z., **Dong, C.-H.**, **Lee, H.**, **Zhu, J.**, **Xiong, L.**, **Gong, D.** ***et al.*** (2005) A DEAD box RNA helicase is essential for mRNA export and important for development and stress responses in Arabidopsis. *The Plant Cell*, **17**, 256–267.

Goode, J.A., **Stead, A.D.**, **Ligrone, R.** & **Duckeit, J.G.** (1994) Studies of protonemal morphogenesis in mosses IV. Aloina (Pottiales). *Journal of Bryology*, **18**, 27–41.

Goodstein, D.M., **Shu, S.**, **Howson, R.**, **Neupane, R.**, **Hayes, R.D.**, **Fazo, J.** ***et al.*** (2012) Phytozome: a comparative platform for green plant genomics. *Nucleic Acids Research*, **40**, D1178–D1186.

Grelet, J., **Benamar, A.**, **Teyssier, E.**, **Avelange-Macherel, M.-H.**, **Grunwald, D.** & **Macherel, D.** (2005) Identification in pea seed mitochondria of a late-embryogenesis abundant protein able to protect enzymes from drying. *Plant Physiology*, **137**, 157–167.

Guzha, A., **McGee, R.**, **Scholz, P.**, **Hartken, D.**, **Lüdke, D.**, **Bauer, K.** ***et al.*** (2022) Cell wall-localized BETA-XYLOSIDASE4 contributes to immunity of Arabidopsis against *Botrytis cinerea*. *Plant Physiology*, **189**, 1794–1813.

Guzha, A., **Whitehead, P.**, **Ischebeck, T.** & **Chapman, K.D.** (2023) Lipid droplets: packing hydrophobic molecules within the aqueous cytoplasm. *Annual Review of Plant Biology*, **74**, 195–223.

Hanano, A., **Blée, E.** & **Murphy, D.J.** (2023) Caleosin/Peroxygenases: multifunctional proteins in plants. *Annals of Botany*, **131**, 387–409.

Hand, S.C., **Menze, M.A.**, **Toner, M.**, **Boswell, L.** & **Moore, D.** (2011) LEA proteins during water stress: not just for plants anymore. *Annual Review of Physiology*, **73**, 115–134.

Hause, B., **Weichert, H.**, **Höhne, M.**, **Kindl, H.** & **Feussner, I.** (2000) Expression of cucumber lipid-body lipoxygenase in transgenic tobacco: lipid-body lipoxygenase is correctly targeted to seed lipid bodies. *Planta*, **210**, 708–714.

Herburger, K., **Lewis, L.A.** & **Holzinger, A.** (2015) Photosynthetic efficiency, desiccation tolerance and ultrastructure in two phylogenetically distinct strains of alpine *Zygnema* sp. (Zygnematophyceae, Streptophyta): role of pre-akinete formation. *Protoplasma*, **252**, 571–589.

Hibshman, J.D. & **Goldstein, B.** (2021) LEA motifs promote desiccation tolerance in vivo. *BMC Biology*, **19**, 263.

Hiss, M., **Meyberg, R.**, **Westermann, J.**, **Haas, F.B.**, **Schneider, L.**, **Schallenberg-Rüdinger, M.** ***et al.*** (2017) Sexual reproduction, sporophyte development and molecular variation in the model moss *Physcomitrella patens*: introducing the ecotype Reute. *The Plant Journal*, **90**, 606–620.

Hoang, D.T., **Chernomor, O.**, **von Haeseler, A.**, **Minh, B.Q.** & **Vinh, L.S.** (2018) UFBoot2: improving the ultrafast bootstrap approximation. *Molecular Biology and Evolution*, **35**, 518–522.

Hori, K., **Maruyama, F.**, **Fujisawa, T.**, **Togashi, T.**, **Yamamoto, N.**, **Seo, M.** ***et al.*** (2014) Klebsormidium flaccidum genome reveals primary factors for plant terrestrial adaptation. *Nature Communications*, **5**, 3978.

Horn, P.J., **Chapman, K.D.** & **Ischebeck, T.** (2021) Isolation of lipid droplets for protein and lipid analysis. In: Bartels, D. & Dörmann, P. (Eds.) *Plant lipids: methods and protocols. Methods in molecular biology*. New York, NY: Springer US, pp. 295–320.

Huang, A.H.C. (1992) Oil bodies and oleosins in seeds. *Annual Review of Plant Biology*, **43**, 177–200.

Huang, C.-Y., **Chung, C.-I.**, **Lin, Y.-C.**, **Hsing, Y.-I.C.** & **Huang, A.H.C.** (2009) Oil bodies and oleosins in *Physcomitrella* possess characteristics representative of early trends in evolution. *Plant Physiology*, **150**, 1192–1203.

Hundertmark, M., **Dimova, R.**, **Lengefeld, J.**, **Seckler, R.** & **Hincha, D.K.** (2011) The intrinsically disordered late embryogenesis abundant protein LEA18 from *Arabidopsis thaliana* modulates membrane stability through

binding and folding. *Biochimica et Biophysica Acta (BBA) - Biomembranes*, **1808**, 446–453.

Hundertmark, M. & **Hincha, D.K.** (2008) LEA (Late Embryogenesis Abundant) proteins and their encoding genes in Arabidopsis thaliana. *BMC Genomics*, **9**, 118.

Irisarri, I., **Darienko, T.**, **Pröschold, T.**, **Fürst-Jansen, J.M.R.**, **Jamy, M.** & **de Vries, J.** (2021) Unexpected cryptic species among streptophyte algae most distant to land plants. *Proceedings of the Royal Society B: Biological Sciences*, **288**, 20212168.

Ischebeck, T. (2016) Lipids in pollen — they are different. *Biochimica et Biophysica Acta (BBA) - Molecular and Cell Biology of Lipids*, **1861**, 1315–1328.

Ischebeck, T., **Krawczyk, H.E.**, **Mullen, R.T.**, **Dyer, J.M.** & **Chapman, K.D.** (2020) Lipid droplets in plants and algae: distribution, formation, turnover and function. *Seminars in Cell & Developmental Biology*, **108**, 82–93.

Ischebeck, T., **Valledor, L.**, **Lyon, D.**, **Gingl, S.**, **Nagler, M.**, **Meijón, M.** ***et al.*** (2014) Comprehensive cell-specific protein analysis in early and late pollen development from diploid microsporocytes to pollen tube growth. *Molecular & Cellular Proteomics*, **13**, 295–310.

Jiang, Z., **Xu, G.**, **Jing, Y.**, **Tang, W.** & **Lin, R.** (2016) Phytochrome B and REVEILLE1/2-mediated signalling controls seed dormancy and germination in Arabidopsis. *Nature Communications*, **7**, 12377.

Jiao, C., **Sørensen, I.**, **Sun, X.**, **Sun, H.**, **Behar, H.**, **Alseekh, S.** ***et al.*** (2020) The *Penium margaritaceum* genome: hallmarks of the origins of land plants. *Cell*, **181**, 1097–1111.e12.

Kalyaanamoorthy, S., **Minh, B.Q.**, **Wong, T.K.F.**, **von Haeseler, A.** & **Jermiin, L.S.** (2017) ModelFinder: fast model selection for accurate phylogenetic estimates. *Nature Methods*, **14**, 587–589.

Katoh, K. & **Standley, D.M.** (2013) MAFFT multiple sequence alignment software version 7: improvements in performance and usability. *Molecular Biology and Evolution*, **30**, 772–780.

Kehelpannala, C., **Rupasinghe, T.**, **Pasha, A.**, **Esteban, E.**, **Hennessy, T.**, **Bradley, D.** ***et al.*** (2021) An Arabidopsis lipid map reveals differences between tissues and dynamic changes throughout development. *The Plant Journal*, **107**, 287–302.

Kelly, A.A., **Quettier, A.-L.**, **Shaw, E.** & **Eastmond, P.J.** (2011) Seed storage oil mobilization is important but not essential for germination or seedling establishment in Arabidopsis. *Plant Physiology*, **157**, 866–875.

Kenrick, P. (2017) How land plant life cycles first evolved. *Science*, **358**, 1538–1539.

Khandelwal, A., **Cho, S.H.**, **Marella, H.**, **Sakata, Y.**, **Perroud, P.-F.**, **Pan, A.** ***et al.*** (2010) Role of ABA and ABI3 in desiccation tolerance. *Science*, **327**, 546.

Klepikova, A.V., **Kasianov, A.S.**, **Gerasimov, E.S.**, **Logacheva, M.D.** & **Penin, A.A.** (2016) A high resolution map of the *Arabidopsis thaliana* developmental transcriptome based on RNA-seq profiling. *The Plant Journal*, **88**, 1058–1070.

Kovacs, D., **Kalmar, E.**, **Torok, Z.** & **Tompa, P.** (2008) Chaperone activity of ERD10 and ERD14, two disordered stress-related plant proteins. *Plant Physiology*, **147**, 381–390.

Krawczyk, H.E., **Rotsch, A.H.**, **Herrfurth, C.**, **Scholz, P.**, **Shomroni, O.**, **Salinas-Riester, G.** ***et al.*** (2022) Heat stress leads to rapid lipid remodeling and transcriptional adaptations in *Nicotiana tabacum* pollen tubes. *Plant Physiology*, **189**, 490–515.

Kretzschmar, F.K., **Doner, N.M.**, **Krawczyk, H.E.**, **Scholz, P.**, **Schmitt, K.**, **Valerius, O.** ***et al.*** (2020) Identification of low-abundance lipid droplet proteins in seeds and seedlings. *Plant Physiology*, **182**, 1326–1345.

Kretzschmar, F.K., **Mengel, L.A.**, **Müller, A.O.**, **Schmitt, K.**, **Blersch, K.F.**, **Valerius, O.** ***et al.*** (2018) PUX10 is a lipid droplet-localized scaffold protein that interacts with CELL DIVISION CYCLE48 and is involved in the degradation of lipid droplet proteins. *Plant Cell*, **30**, 2137–2160.

Lamesch, P., **Berardini, T.Z.**, **Li, D.**, **Swarbreck, D.**, **Wilks, C.**, **Sasidharan, R.** ***et al.*** (2012) The Arabidopsis information resource (TAIR): improved gene annotation and new tools. *Nucleic Acids Research*, **40**, D1202–D1210.

Lang, D., **Ullrich, K.K.**, **Murat, F.**, **Fuchs, J.**, **Jenkins, J.**, **Haas, F.B.** ***et al.*** (2018) The *Physcomitrella patens* chromosome-scale assembly reveals moss genome structure and evolution. *The Plant Journal*, **93**, 515–533.

Leebens-Mack, J.H., **Barker, M.S.**, **Carpenter, E.J.** ***et al.*** (2019) One thousand plant transcriptomes and the phylogenomics of green plants. *Nature*, **574**, 679–685.

Leprince, O., **van Aelst, A.C.**, **Pritchard, H.W.** & **Murphy, D.J.** (1997) Oleosins prevent oil-body coalescence during seed imbibition as suggested by a low-temperature scanning electron microscope study of desiccation-tolerant and -sensitive oilseeds. *Planta*, **204**, 109–119.

Letunic, I. & **Bork, P.** (2007) Interactive Tree Of Life (iTOL): an online tool for phylogenetic tree display and annotation. *Bioinformatics*, **23**, 127–128.

Leubner-Metzger, G. (2003) Brassinosteroids promote seed germination. In: Hayat, S. & Ahmad, A. (Eds.) *Brassinosteroids: bioactivity and crop productivity*. Dordrecht: Springer Netherlands, pp. 119–128.

Li, F., **Asami, T.**, **Wu, X.**, **Tsang, E.W.T.** & **Cutler, A.J.** (2007) A putative hydroxysteroid dehydrogenase involved in regulating plant growth and development. *Plant Physiology*, **145**, 87–97.

Li, F.-W., **Brouwer, P.**, **Carretero-Paulet, L.**, **Cheng, S.**, **de Vries, J.**, **Delaux, P.M.** ***et al.*** (2018) Fern genomes elucidate land plant evolution and cyanobacterial symbioses. *Nature Plants*, **4**, 460–472.

Li, F.-W., **Nishiyama, T.**, **Waller, M.**, **Frangedakis, E.**, **Keller, J.**, **Li, Z.** ***et al.*** (2020) Anthoceros genomes illuminate the origin of land plants and the unique biology of hornworts. *Nature Plants*, **6**, 259–272.

Li, S., **Chakraborty, N.**, **Borcar, A.**, **Menze, M.A.**, **Toner, M.** & **Hand, S.C.** (2012) Late embryogenesis abundant proteins protect human hepatoma cells during acute desiccation. *Proceedings of the National Academy of Sciences of the United States of America*, **109**, 20859–20864.

Li, Z., **Wu, S.**, **Chen, J.**, **Wang, X.**, **Gao, J.**, **Ren, G.** ***et al.*** (2017) NYEs/SGRs-mediated chlorophyll degradation is critical for detoxification during seed maturation in Arabidopsis. *The Plant Journal*, **92**, 650–661.

Ligrone, R., **Duckett, J.G.** & **Renzaglia, K.S.** (2012) Major transitions in the evolution of early land plants: a bryological perspective. *Annals of Botany*, **109**, 851–871.

Lin, L.-J., **Tai, S.S.K.**, **Peng, C.-C.** & **Tzen, J.T.C.** (2002) Steroleosin, a sterol-binding dehydrogenase in seed oil bodies. *Plant Physiology*, **128**, 1200–1211.

Liu, X., **Wang, Z.**, **Wang, L.**, **Wu, R.**, **Phillips, J.** & **Deng, X.** (2009) LEA 4 group genes from the resurrection plant *Boea hygrometrica* confer dehydration tolerance in transgenic tobacco. *Plant Science*, **176**, 90–98.

Loconte, H. & **Stevenson, D.W.** (1990) Cladistics of the Spermatophyta. *Brittonia*, **42**, 197–211.

López-Pozo, M., **Fernández-Marín, B.**, **García-Plazaola, J.I.** & **Ballesteros, D.** (2018) Desiccation tolerance in ferns: from the unicellular spore to the multi-tissular sporophyte. In: Fernández, H. (Ed.) *Current advances in fern research*. Cham: Springer International Publishing, pp. 401–426.

Luo, W., **Komatsu, S.**, **Abe, T.**, **Matsuura, H.** & **Takahashi, K.** (2020) Comparative proteomic analysis of wild-type *Physcomitrella patens* and an OPDA-deficient *Physcomitrella patens* mutant with disrupted PpAOS1 and PpAOS2 genes after wounding. *International Journal of Molecular Sciences*, **21**, 1417.

Lyall, R. & **Gechev, T.** (2020) Multi-omics insights into the evolution of angiosperm resurrection plants. In: Roberts, J.A. (Ed.) *Annual plant reviews online*. Hoboken, New Jersey, USA: John Wiley & Sons, Ltd, pp. 77–110.

Mamaeva, A., **Knyazev, A.**, **Glushkevich, A.** & **Fesenko, I.** (2022) Quantitative proteomic dataset of the moss *Physcomitrium patens* PSEP3 KO and OE mutant lines. *Data in Brief*, **40**, 107715.

Manfre, A.J., **LaHatte, G.A.**, **Climer, C.R.** & **Marcotte, W.R.** (2008) Seed dehydration and the establishment of desiccation tolerance during seed maturation is altered in the *Arabidopsis thaliana* mutant atem6-1. *Plant and Cell Physiology*, **50**, 243–253.

Marchant, D.B., **Chen, G.**, **Cai, S.**, **Chen, F.**, **Schafran, P.**, **Jenkins, J.** ***et al.*** (2022) Dynamic genome evolution in a model fern. *Nature Plants*, **8**, 1038–1051.

Matilla, A.J. (2022) The orthodox dry seeds are alive: a clear example of desiccation tolerance. *Plants*, **11**, 20.

Matsui, K., **Hijiya, K.**, **Tabuchi, Y.** & **Kajiwara, T.** (1999) Cucumber cotyledon lipoxygenase during postgerminative growth. Its expression and action on lipid bodies. *Plant Physiology*, **119**, 1279–1288.

McLean, R.J. & **Pessoney, G.F.** (1971) Formation and resistance of akinetes of Zygnema. In: Parker, B.C. & Brown, R.M., Jr. (Eds.) *Contributions in phycology*. Lawrence, Kansas, USA: Allen Press, pp. 145–152.

Merchant, S.S., **Prochnik, S.E.**, **Vallon, O.**, **Harris, E.H.**, **Karpowicz, S.J.**, **Witman, G.B.** ***et al.*** (2007) The Chlamydomonas genome reveals the evolution of key animal and plant functions. *Science*, **318**, 245–250.

Minh, B.Q., **Schmidt, H.A.**, **Chernomor, O.**, **Schrempf, D.**, **Woodhams, M.D.**, **von Haeseler, A.** ***et al.*** (2020) IQ-TREE 2: new models and efficient

methods for phylogenetic inference in the genomic era. *Molecular Biology and Evolution*, **37**, 1530–1534.

Moody, L.A., **Saidi, Y.**, **Gibbs, D.J.**, **Choudhary, A.**, **Holloway, D.**, **Vesty, E.F.** ***et al.*** (2016) An ancient and conserved function for armadillo-related proteins in the control of spore and seed germination by abscisic acid. *New Phytologist*, **211**, 940–951.

Morikawa, T., **Saga, H.**, **Hashizume, H.** & **Ohta, D.** (2009) CYP710A genes encoding sterol C22-desaturase in *Physcomitrella patens* as molecular evidence for the evolutionary conservation of a sterol biosynthetic pathway in plants. *Planta*, **229**, 1311–1322.

Müller, A.O. & **Ischebeck, T.** (2018) Characterization of the enzymatic activity and physiological function of the lipid droplet-associated triacylglycerol lipase AtOBL1. *New Phytologist*, **217**, 1062–1076.

Murphy, D.J., **Ross, J.H.** & **Pritchard, H.W.** (1995) Are oleosins only associated with oil bodies from desiccation tolerant plant tissues? In: Kader, J.C. & Mazliak, P. (Eds.) *Plant lipid metabolism*, Dordrecht, Netherlands: Springer, pp. 558–560.

Nakosteen, P.C. & **Hughes, K.W.** (1978) Sexual life cycle of three species of funariaceae in culture. *The Bryologist*, **81**, 307–314.

Niemeyer, P.W., **Irisarri, I.**, **Scholz, P.**, **Schmitt, K.**, **Valerius, O.**, **Braus, G.H.** ***et al.*** (2022) A seed-like proteome in oil-rich tubers. *The Plant Journal*, **112**, 518–534.

Nietzel, T., **Mostertz, J.**, **Ruberti, C.**, **Née, G.**, **Fuchs, P.**, **Wagner, S.** ***et al.*** (2020) Redox-mediated kick-start of mitochondrial energy metabolism drives resource-efficient seed germination. *Proceedings of the National Academy of Sciences of the United States of America*, **117**, 741–751.

Nishiyama, T., **Sakayama, H.**, **de Vries, J.**, **Buschmann, H.**, **Saint-Marcoux, D.**, **Ullrich, K.K.** ***et al.*** (2018) The Chara genome: secondary complexity and implications for plant terrestrialization. *Cell*, **174**, 448–464.e24.

Nonogaki, H. (2014) Seed dormancy and germination—emerging mechanisms and new hypotheses. *Frontiers in Plant Science*, **5**, 233.

Nystedt, B., **Street, N.R.**, **Wetterbom, A.**, **Zuccolo, A.**, **Lin, Y.C.**, **Scofield, D.G.** ***et al.*** (2013) The Norway spruce genome sequence and conifer genome evolution. *Nature*, **497**, 579–584.

Oliver, M.J., **Farrant, J.M.**, **Hilhorst, H.W.M.**, **Mundree, S.**, **Williams, B.** & **Bewley, J.D.** (2020) Desiccation tolerance: avoiding cellular damage during drying and rehydration. *Annual Review of Plant Biology*, **71**, 435–460.

Oliver, M.J., **Tuba, Z.** & **Mishler, B.D.** (2000) The evolution of vegetative desiccation tolerance in land plants. *Plant Ecology*, **151**, 85–100.

Oliver, M.J., **Velten, J.** & **Mishler, B.D.** (2005) Desiccation tolerance in bryophytes: a reflection of the primitive strategy for plant survival in dehydrating habitats? *Integrative and Comparative Biology*, **45**, 788–799.

Ouyang, S., **Zhu, W.**, **Hamilton, J.**, **Lin, H.**, **Campbell, M.**, **Childs, K.** ***et al.*** (2007) The TIGR Rice Genome Annotation Resource: improvements and new features. *Nucleic Acids Research*, **35**, D883–D887.

Pacini, E. (2012) Pollen and seed analogies. *Plant Biosystems - An International Journal Dealing with all Aspects of Plant Biology*, **146**, 738–748.

Peres, A.L.G.L., **Soares, J.S.**, **Tavares, R.G.**, **Righetto, G.**, **Zullo, M.A.T.**, **Mandava, N.B.** ***et al.*** (2019) Brassinosteroids, the sixth class of phytohormones: a molecular view from the discovery to hormonal interactions in plant development and stress adaptation. *International Journal of Molecular Sciences*, **20**, 331.

Permann, C., **Gierlinger, N.** & **Holzinger, A.** (2022) Zygospores of the green alga Spirogyra: new insights from structural and chemical imaging. *Frontiers in Plant Science*, **13**, 1080111.

Permann, C., **Herburger, K.**, **Niedermeier, M.**, **Felhofer, M.**, **Gierlinger, N.** & **Holzinger, A.** (2021) Cell wall characteristics during sexual reproduction of *Mougeotia* sp. (Zygnematophyceae) revealed by electron microscopy, glycan microarrays and RAMAN spectroscopy. *Protoplasma*, **258**, 1261–1275.

Permann, C., **Pichrtová, M.**, **Šoljaková, T.**, **Herburger, K.**, **Jouneau, P.-H.**, **Uwizeye, C.** ***et al.*** (2023) 3D-reconstructions of zygospores in *Zygnema vaginatum* (Charophyta) reveal details of cell wall formation, suggesting adaptations to extreme habitats. *Physiologia Plantarum*, **175**, e13988.

Perroud, P.-F., **Haas, F.B.**, **Hiss, M.**, **Ullrich, K.K.**, **Alboresi, A.**, **Amirebrahimi, M.** ***et al.*** (2018) The *Physcomitrella patens* gene atlas project: large-scale RNA-seq based expression data. *The Plant Journal*, **95**, 168–182.

Pichrtová, M., **Arc, E.**, **Stöggl, W.**, **Kranner, I.**, **Hájek, T.**, **Hackl, H.** ***et al.*** (2016) Formation of lipid bodies and changes in fatty acid composition upon prekinete formation in Arctic and Antarctic Zygnema (Zygnematophyceae, Streptophyta) strains. *FEMS Microbiology Ecology*, **92**, fiw096.

Pichrtová, M., **Kulichová, J.** & **Holzinger, A.** (2014) Nitrogen limitation and slow drying induce desiccation tolerance in conjugating green algae (Zygnematophyceae, Streptophyta) from polar habitats. *PLoS One*, **9**, e113137.

Puttick, M.N., **Morris, J.L.**, **Williams, T.A.**, **Cox, C.J.**, **Edwards, D.**, **Kenrick, P.** ***et al.*** (2018) The interrelationships of land plants and the nature of the ancestral embryophyte. *Current Biology*, **28**, 733–745.e2.

Pyc, M., **Gidda, S.K.**, **Seay, D.**, **Esnay, N.**, **Kretzschmar, F.K.**, **Cai, Y.** ***et al.*** (2021) LDIP cooperates with SEIPIN and LDAP to facilitate lipid droplet biogenesis in Arabidopsis. *The Plant Cell*, **33**, 3076–3103.

Rappsilber, J., **Mann, M.** & **Ishihama, Y.** (2007) Protocol for micro-purification, enrichment, pre-fractionation and storage of peptides for proteomics using StageTips. *Nature Protocols*, **2**, 1896–1906.

Rensing, S.A. (2018) Great moments in evolution: the conquest of land by plants. *Current Opinion in Plant Biology*, **42**, 49–54.

Rensing, S.A., **Goffinet, B.**, **Meyberg, R.**, **Wu, S.-Z.** & **Bezanilla, M.** (2020) The moss *Physcomitrium* (*Physcomitrella*) *patens*: a model organism for non-seed plants. *Plant Cell*, **32**, 1361–1376.

Rensing, S.A., **Lang, D.**, **Zimmer, A.D.**, **Terry, A.**, **Salamov, A.**, **Shapiro, H.** ***et al.*** (2008) The *Physcomitrella* genome reveals evolutionary insights into the conquest of land by plants. *Science*, **319**, 64–69.

Rowntree, J.K., **Duckett, J.G.**, **Mortimer, C.L.**, **Ramsay, M.M.** & **Pressel, S.** (2007) Formation of specialized propagules resistant to desiccation and cryopreservation in the threatened moss *Ditrichum plumbicola* (Ditrichales, Bryopsida). *Annals of Botany*, **100**, 483–496.

Saavedra, L., **Svensson, J.**, **Carballo, V.**, **Izmendi, D.**, **Welin, B.** & **Vidal, S.** (2006) A dehydrin gene in *Physcomitrella patens* is required for salt and osmotic stress tolerance. *The Plant Journal*, **45**, 237–249.

Sano, N. & **Marion-Poll, A.** (2021) ABA metabolism and homeostasis in seed dormancy and germination. *International Journal of Molecular Sciences*, **22**, 5069.

Sarnighausen, E., **Wurtz, V.**, **Heintz, D.**, **Van Dorsselaer, A.** & **Reski, R.** (2004) Mapping of the *Physcomitrella patens* proteome. *Phytochemistry*, **65**, 1589–1607.

Schnepf, E. & **Reinhard, C.** (1997) Brachycytes in funaria protonemate: induction by abscisic acid and fine structure. *Journal of Plant Physiology*, **151**, 166–175.

Shaw, A.J., **Szövényi, P.** & **Shaw, B.** (2011) Bryophyte diversity and evolution: windows into the early evolution of land plants. *American Journal of Botany*, **98**, 352–369.

Shevchenko, A., **Tomas, H.**, **Havli, J.**, **Olsen, J.V.** & **Mann, M.** (2006) In-gel digestion for mass spectrometric characterization of proteins and proteomes. *Nature Protocols*, **1**, 2856–2860.

Shimada, T.L., **Shimada, T.**, **Takahashi, H.**, **Fukao, Y.** & **Hara-Nishimura, I.** (2008) A novel role for oleosins in freezing tolerance of oilseeds in *Arabidopsis thaliana*. *The Plant Journal*, **55**, 798–809.

Shimada, T.L., **Takano, Y.**, **Shimada, T.**, **Fujiwara, M.**, **Fukao, Y.**, **Mori, M.** ***et al.*** (2014) Leaf oil body functions as a subcellular factory for the production of a phytoalexin in Arabidopsis. *Plant Physiology*, **164**, 105–118.

Siloto, R.M.P., **Findlay, K.**, **Lopez-Villalobos, A.**, **Yeung, E.C.**, **Nykiforuk, C.L.** & **Moloney, M.M.** (2006) The accumulation of oleosins determines the size of seed oilbodies in Arabidopsis. *The Plant Cell*, **18**, 1961–1974.

Skripnikov, A.Y., **Polyakov, N.B.**, **Tolcheva, E.V.**, **Velikodvorskaya, V.V.**, **Dolgov, S.V.**, **Demina, I.A.** ***et al.*** (2009) Proteome analysis of the moss *Physcomitrella patens* (Hedw.) B.S.G. *Biochemistry (Moscow)*, **74**, 480–490.

Sperschneider, J., **Catanzariti, A.-M.**, **DeBoer, K.**, **Petre, B.**, **Gardiner, D.M.**, **Singh, K.B.** ***et al.*** (2017) LOCALIZER: subcellular localization prediction of both plant and effector proteins in the plant cell. *Scientific Reports*, **7**, 44598.

Tian, R., **Wang, F.**, **Zheng, Q.**, **Niza, V.M.A.G.E.**, **Downie, A.B.** & **Perry, S.E.** (2020) Direct and indirect targets of the arabidopsis seed transcription factor ABSCISIC ACID INSENSITIVE3. *The Plant Journal*, **103**, 1679–1694.

Tolleter, D., **Hincha, D.K.** & **Macherel, D.** (2010) A mitochondrial late embryogenesis abundant protein stabilizes model membranes in the dry state. *Biochimica et Biophysica Acta (BBA) - Biomembranes*, **1798**, 1926–1933.

Toshima, E., **Nanjo, Y.**, **Komatsu, S.**, **Abe, T.**, **Matsuura, H.** & **Takahashi, K.** (2014) Proteomic analysis of *Physcomitrella patens* treated with 12-oxo-phytodienoic acid, an important oxylipin in plants. *Bioscience, Biotechnology, and Biochemistry*, **78**, 946–953.

Tyanova, S., **Temu, T.** & **Cox, J.** (2016) The MaxQuant computational platform for mass spectrometry-based shotgun proteomics. *Nature Protocols*, **11**, 2301–2319.

Tyanova, S., **Temu, T.**, **Sinitcyn, P.**, **Carlson, A.**, **Hein, M.Y.**, **Geiger, T.** ***et al.*** (2016) The Perseus computational platform for comprehensive analysis of (prote)omics data. *Nature Methods*, **13**, 731–740.

VanBuren, R., **Wai, C.M.**, **Zhang, Q.**, **Song, X.**, **Edger, P.P.**, **Bryant, D.** ***et al.*** (2017) Seed desiccation mechanisms co-opted for vegetative desiccation in the resurrection grass *Oropetium thomaeum*. *Plant, Cell & Environment*, **40**, 2292–2306.

Vesty, E.F., **Saidi, Y.**, **Moody, L.A.**, **Holloway, D.**, **Whitbread, A.**, **Needs, S.** ***et al.*** (2016) The decision to germinate is regulated by divergent molecular networks in spores and seeds. *The New Phytologist*, **211**, 952–966.

Vizcaíno, J.A., **Deutsch, E.W.**, **Wang, R.**, **Csordas, A.**, **Reisinger, F.**, **Ríos, D.** ***et al.*** (2014) ProteomeXchange provides globally coordinated proteomics data submission and dissemination. *Nature Biotechnology*, **32**, 223–226.

Vogel, J.P., **Garvin, D.F.**, **Mockler, T.C.** ***et al.*** (2010) Genome sequencing and analysis of the model grass *Brachypodium distachyon*. *Nature*, **463**, 763–768.

Vollmeister, E., **Phokas, A.**, **Meyberg, R.**, **Böhm, C.V.**, **Peter, M.**, **Kohnert, E.** ***et al.*** (2023) A DELAY OF GERMINATION 1 (DOG1)-like protein regulates spore germination in the moss *Physcomitrium patens*. *The Plant Journal*. Available from: https://doi.org/10.1111/tpj.16537

Wallace, S., **Fleming, A.**, **Wellman, C.H.** & **Beerling, D.J.** (2011) Evolutionary development of the plant spore and pollen wall. *AoB Plants*, **2011**, plr027.

Wan, T., **Liu, Z.-M.**, **Li, L.-F.**, **Leitch, A.R.**, **Leitch, I.J.**, **Lohaus, R.** ***et al.*** (2018) A genome for gnetophytes and early evolution of seed plants. *Nature Plants*, **4**, 82–89.

Wang, S., **Li, L.**, **Li, H.**, **Sahu, S.K.**, **Wang, H.**, **Xu, Y.** ***et al.*** (2020) Genomes of early-diverging streptophyte algae shed light on plant terrestrialization. *Nature Plants*, **6**, 95–106.

Wang, X., **Kuang, T.** & **He, Y.** (2010) Conservation between higher plants and the moss *Physcomitrella patens* in response to the phytohormone abscisic acid: a proteomics analysis. *BMC Plant Biology*, **10**, 192.

Wang, X., **Yang, P.**, **Gao, Q.**, **Liu, X.**, **Kuang, T.**, **Shen, S.** ***et al.*** (2008) Proteomic analysis of the response to high-salinity stress in *Physcomitrella patens*. *Planta*, **228**, 167–177.

Wang, X., **Yang, P.**, **Zhang, X.**, **Xu, Y.**, **Kuang, T.**, **Shen, S.** ***et al.*** (2009) Proteomic analysis of the cold stress response in the moss, *Physcomitrella patens*. *Proteomics*, **9**, 4529–4538.

Wang, X.Q., **Yang, P.F.**, **Liu, Z.**, **Liu, W.Z.**, **Hu, Y.**, **Chen, H.** ***et al.*** (2009) Exploring the mechanism of *Physcomitrella patens* desiccation tolerance through a proteomic strategy. *Plant Physiology*, **149**, 1739–1750.

Waters, E.R. & **Vierling, E.** (2020) Plant small heat shock proteins – evolutionary and functional diversity. *New Phytologist*, **227**, 24–37.

Wester, L., **Somers, D.E.**, **Clack, T.** & **Sharrock, R.A.** (1994) Transgenic complementation of the *hy3* phytochrome B mutation and response to PHYB gene copy number in Arabidopsis. *The Plant Journal*, **5**, 261–272.

Wickell, D., **Kuo, L.-Y.**, **Yang, H.-P.**, **Dhabalia Ashok, A.**, **Irisarri, I.**, **Dadras, A.** ***et al.*** (2021) Underwater CAM photosynthesis elucidated by Isoetes genome. *Nature Communications*, **12**, 6348.

Wolkers, W.F., **McCready, S.**, **Brandt, W.F.**, **Lindsey, G.G.** & **Hoekstra, F.A.** (2001) Isolation and characterization of a D-7 LEA protein from pollen that stabilizes glasses in vitro. *Biochimica et Biophysica Acta (BBA) - Protein Structure and Molecular Enzymology*, **1544**, 196–206.

Xia, L., **Zou, D.**, **Sang, J.**, **Xu, X.**, **Yin, H.**, **Li, M.** ***et al.*** (2017) Rice expression database (RED): an integrated RNA-seq-derived gene expression database for rice. *Journal of Genetics and Genomics*, **44**, 235–241.

Xiong, M., **Yu, J.**, **Wang, J.**, **Gao, Q.**, **Huang, L.**, **Chen, C.** ***et al.*** (2022) Brassinosteroids regulate rice seed germination through the BZR1-RAmy3D transcriptional module. *Plant Physiology*, **189**, 402–418.

Xu, Z., **Xin, T.**, **Bartels, D.**, **Li, Y.**, **Gu, W.**, **Yao, H.** ***et al.*** (2018) Genome analysis of the ancient tracheophyte *Selaginella tamariscina* reveals evolutionary features relevant to the acquisition of desiccation tolerance. *Molecular Plant*, **11**, 983–994.

Yadav, M.K. & **Bhatla, S.C.** (2011) Localization of lipoxygenase activity on the oil bodies and in protoplasts using a novel fluorescence imaging method. *Plant Physiology and Biochemistry*, **49**, 230–234.

Yamauchi, Y., **Hasegawa, A.**, **Taninaka, A.**, **Mizutani, M.** & **Sugimoto, Y.** (2011) NADPH-dependent reductases involved in the detoxification of reactive carbonyls in plants. *Journal of Biological Chemistry*, **286**, 6999–7009.

Yang, Z., **Ji, H.** & **Liu, D.** (2016) Oil biosynthesis in underground oil-rich storage vegetative tissue: comparison of *Cyperus esculentus* tuber with oil seeds and fruits. *Plant & Cell Physiology*, **57**, 2519–2540.

Yang, Z., **Liu, X.**, **Wang, K.**, **Li, Z.**, **Jia, Q.**, **Zhao, C.** ***et al.*** (2022) ABA-INSENSITIVE 3 with or without FUSCA3 highly up-regulates lipid droplet proteins and activates oil accumulation. *Journal of Experimental Botany*, **73**, 2077–2092.

Yao, L., **Cheng, X.**, **Gu, Z.**, **Huang, W.**, **Li, S.**, **Wang, L.** ***et al.*** (2018) The AWPM-19 family protein OsPM1 mediates abscisic acid influx and drought response in rice. *The Plant Cell*, **30**, 1258–1276.

Yokota, T., **Ohnishi, T.**, **Shibata, K.**, **Asahina, M.**, **Nomura, T.**, **Fujita, T.** ***et al.*** (2017) Occurrence of brassinosteroids in non-flowering land plants, liverwort, moss, lycophyte and fern. *Phytochemistry*, **136**, 46–55.

Yotsui, I., **Serada, S.**, **Naka, T.**, **Saruhashi, M.**, **Taji, T.**, **Hayashi, T.** ***et al.*** (2016) Large-scale proteome analysis of abscisic acid and ABSCISIC ACID INSENSITIVE3-dependent proteins related to desiccation tolerance in *Physcomitrella patens*. *Biochemical and Biophysical Research Communications*, **471**, 589–595.

Zienkiewicz, A., **Zienkiewicz, K.**, **Rejón, J.D.**, **Alché Jde, D.**, **Castro, A.J.** & **Rodríguez-García, M.I.** (2014) Olive seed protein bodies store degrading enzymes involved in mobilization of oil bodies. *Journal of Experimental Botany*, **65**, 103–115.

Zienkiewicz, A., **Zienkiewicz, K.**, **Rejón, J.D.**, **Rodríguez-García, M.I.** & **Castro, A.J.** (2013) New insights into the early steps of oil body mobilization during pollen germination. *Journal of Experimental Botany*, **64**, 293–302.